

DO WE NEED REBALANCING STRATEGIES? A THEORETICAL AND EMPIRICAL STUDY AROUND SMOTE AND ITS VARIANTS

Anonymous authors

Paper under double-blind review

ABSTRACT

Synthetic Minority Oversampling Technique (SMOTE) is a common rebalancing strategy for handling imbalanced tabular data sets. However, few works analyze SMOTE theoretically. In this paper, we prove that SMOTE (with default parameter) tends to copies the original minority samples asymptotically. We also prove that SMOTE exhibits boundary artifacts, thus justifying existing SMOTE variants. Then we introduce two new SMOTE-related strategies, and compare them with state-of-the-art rebalancing procedures. Surprisingly, for most data sets, we observe that applying no rebalancing strategy is competitive in terms of predictive performances, with tuned random forests, logistic regression or LightGBM. For highly imbalanced data sets, our new methods, named CV-SMOTE and Multivariate Gaussian SMOTE, are competitive. Besides, our analysis sheds some lights on the behavior of common rebalancing strategies, when used in conjunction with random forests.

1 INTRODUCTION

Imbalanced data sets for binary classification are encountered in various fields such as fraud detection (Hassan & Abraham, 2016), medical diagnosis (Khalilia et al., 2011) and even churn detection (Nguyen & Duong, 2021). In our study, we focus on imbalanced data in the context of binary classification on tabular data, for which most machine learning algorithms have a tendency to predict the majority class. This leads to biased predictions, so that several rebalancing strategies have been developed in order to handle this issue, as explained by Krawczyk (2016) and Ramyachitra & Manikandan (2014). These procedures can be divided into two categories: model-level and data-level.

Model-level approaches modify existing classifiers in order to prevent predicting only the majority class. Among such techniques, Class-Weight (CW) works by assigning higher weights to minority samples. Another related proposed by Zhu et al. (2018) assigns data-driven weights to each tree of a random forest, in order to improve aggregated metrics such as F1 score or ROC AUC. Another model-level technique is to modify the loss function of the classifier. For instance, Cao et al. (2019) and Lin et al. (2017) introduced two new losses, respectively LDAM and Focal losses, in order to produce neural network classifiers that better handle imbalanced data sets. However, model-level approaches are not model agnostic, and thus cannot be applied to a wide variety of machine learning algorithms. Consequently, we focus in this paper on data-level approaches.

Data-level approaches can be divided into two groups: synthetic and non-synthetic procedures. Non-synthetic procedures works by removing or copying original data points. Mani & Zhang (2003) explain that Random Under Sampling (RUS) is one of the most used resampling strategy and design new adaptive versions called Nearmiss. RUS produces the prespecified balance between classes by dropping uniformly at random majority class samples. The Nearmiss1 strategy (Mani & Zhang, 2003) includes a distinction between majority samples by ranking them with their mean distance to their nearest neighbor from the minority class. Then, low-ranked majority samples are dropped until a given balancing ratio is reached. In contrast, Random Over Sampling (ROS) duplicates original minority samples. The main limitation of all these sampling strategies is the fact that they either remove information from the data or do not add new information.

On the contrary, synthetic procedures generate new synthetic samples in the minority class. One of the most famous strategies in this group is *Synthetic Minority Oversampling Technique* (SMOTE, see Chawla et al., 2002)¹. In SMOTE, new minority samples are generated via linear interpolation between an original minority sample and one of its nearest neighbor in the minority class. Other approaches are based on Generative Adversarial Networks (GAN Islam & Zhang, 2020), which are computationally expensive and mostly designed for specific data structures, such as images. Random Over Sampling Examples (see Menardi & Torelli, 2014) is a variant of ROS that produces duplicated samples and then add a noise in order to get these samples slightly different from the original ones. This leads to the generation of new samples on the neighborhood of original minority samples. The main difficulty of these strategies is to synthesize relevant new samples, which must not be outliers nor simple copies of original points.

Contributions We place ourselves in the setting of imbalanced classification on tabular data, which is very common in real-world applications (see Shwartz-Ziv & Armon, 2022). In this paper:

- We prove that, without tuning the hyperparameter K (usually set to 5), SMOTE asymptotically copies the original minority samples, therefore lacking the intrinsic variability required in any synthetic generative procedure. We provide numerical illustrations of this limitation (Section 3).
- We also establish that SMOTE density vanishes near the boundary of the support of the minority distribution, therefore justifying the introduction of SMOTE variants such as BorderLine SMOTE (Section 3).
- Our theoretical analysis naturally leads us to introduce two SMOTE alternatives, CV-SMOTE and Multivariate Gaussian SMOTE (MGS). In Section 4, we evaluate our new strategies and state-of-the-art rebalancing strategies on several real-world data sets using random forests/logistic regression/LightGBM. Through these experiments ² we show that applying no strategy is competitive for most data sets. For the remaining data sets, our proposed strategies, CV-SMOTE and MGS, are among the best strategies in terms of predictive performances. Our analysis also provides some explanations about the good behavior of RUS, due to an implicit regularization in presence of random forests classifiers.

2 RELATED WORKS

In this section, we focus on the literature that is the most relevant to our work: long-tail learning, SMOTE variants and theoretical studies of rebalancing strategies.

Long-tailed learning (see, e.g., Zhang et al., 2023) is a relatively new field, originally designed to handle image classification with numerous output classes. Most techniques in long-tailed learning are based on neural networks or use the large number of classes to build or adapt aggregated predictors. However, in most tabular classification data sets, the number of classes to predict is relatively small, usually equal to two (Chawla et al., 2004; He & Garcia, 2009; Grinsztajn et al., 2022). Therefore, long-tailed learning methods are not intended for our setting as (i) we only have two output classes and (ii) state-of-the-art models for tabular data are not neural networks but tree-based methods, such as random forests or gradient boosting (see Grinsztajn et al., 2022; Shwartz-Ziv & Armon, 2022).

SMOTE has seen many variants proposed in the literature. Several of them focus on generating synthetic samples near the boundary of the minority class support, such as ADASYN (He et al., 2008), SVM-SMOTE (Nguyen et al., 2011) or Borderline SMOTE (Han et al., 2005). Many other variants exist such as SMOTEBoost (Chawla et al., 2003), Adaptive-SMOTE (Pan et al., 2020), Xie et al. (2020) or DBSMOTE (Bunkhumpornpat et al., 2012). From a computational perspective, several synthetic methods are available in the open-source package *imb-learn* (see Lemaître et al., 2017). Several papers study experimentally some specificities of the sampling strategies and the impact of hyperparameter tuning. For example, Kamalov et al. (2022) study the optimal sampling ratio for imbalanced data sets when using synthetic approaches. Aguiar et al. (2023) realize a survey

¹More than 25.000 papers found in GoogleScholar with a title including “SMOTE” over the last decade.

²All our experiments and our newly proposed methods can be found at https://github.com/anonymous8880/smote_study.

on imbalance data sets in the context of online learning and propose a standardized framework in order to compare rebalancing strategies in this context. Furthermore, Wongvorachan et al. (2023) aim at comparing the synthetic approaches (ROS, RUS and SMOTE) on educational data.

Several works study theoretically the rebalancing strategies. Xu et al. (2020) study the weighted risk of plug-in classifiers, for arbitrary weights. They establish rates of convergence and derive a new robust risk that may in turn improve classification performance in imbalanced scenarios. Then, based on this previous work, Aghbalou et al. (2024) derive a sharp error bound of the balanced risk for binary classification context with severe class imbalance. Using extreme value theory, Chaudhuri et al. (2023) show that applying Random Under Sampling in binary classification framework improve the worst-group error when learning from imbalanced classes with tails. Wallace & Dahabreh (2014) study the class probability estimates for several rebalancing strategies before introducing a generic methodology in order to improve all these estimates. Dal Pozzolo et al. (2015) focus on the effect of RUS on the posterior probability of the selected classifier. They show that RUS affect the accuracy and the probability calibration of the model. To the best of our knowledge, there are only few theoretical works dissecting the intrinsic machinery in SMOTE algorithm, with the notable exception of Elreedy & Atiya (2019) and Elreedy et al. (2023) who established the density of synthetic observations generated by SMOTE, the associated expectation and covariance matrix.

3 A STUDY OF SMOTE

Notations We denote by $\mathcal{U}([a, b])$ the uniform distribution over $[a, b]$. We denote by $\mathcal{N}(\mu, \Sigma)$ the multivariate normal distribution of mean $\mu \in \mathbb{R}^d$ and covariance matrix $\Sigma \in \mathbb{R}^{d \times d}$. For any set A , we denote by $Vol(A)$, the Lebesgue measure of A . For any $z \in \mathbb{R}^d$ and $r > 0$, let $B(z, r)$ be the ball centered at z of radius r . We note $c_d = Vol(B(0, 1))$ the volume of the unit ball in \mathbb{R}^d . For any $p, q \in \mathbb{N}$, and any $z \in [0, 1]$, we denote by $\mathcal{B}(p, q; z) = \int_{t=0}^z t^{p-1}(1-t)^{q-1} dt$ the incomplete beta function.

3.1 SMOTE ALGORITHM

We assume to be given a training sample composed of (X_i, Y_i) N pairs independent and identically distributed as (X, Y) , where X and Y are random variables that take values respectively in $\mathcal{X} \subset \mathbb{R}^d$ and $\{0, 1\}$. We consider a class imbalance problem, in which the class $Y = 1$ is under-represented, compared to the class $Y = 0$, and thus called the minority class. We assume that we have n minority samples in our training set. We define the imbalance ratio as n/N . In this paper, we consider continuous input variables only, as SMOTE was originally designed such variables only.

Algorithm 1 SMOTE iteration.

Input: Minority class samples X_1, \dots, X_n , number K of nearest-neighbors
 Select uniformly at random X_c (called **central point**) among X_1, \dots, X_n .
 Denote by I the set composed of the K nearest-neighbors of X_c among X_1, \dots, X_n (w.r.t. L_2 norm).
 Select $X_k \in I$ uniformly.
 Sample $w \sim \mathcal{U}([0, 1])$
 $Z_{K,n} \leftarrow X_c + w(X_k - X_c)$
Return $Z_{K,n}$

In this section, we study the SMOTE procedure, which generates synthetic data through linear interpolations between two pairs of original samples of the minority class. SMOTE algorithm has a single hyperparameter, K , by default set to 5, which stands for the number of nearest neighbors considered when interpolating. A single SMOTE iteration is detailed in Algorithm 1. In a classic machine learning pipeline, SMOTE procedure is repeated in order to obtain a prespecified ratio between the two classes, before training a classifier.

3.2 THEORETICAL RESULTS ON SMOTE

SMOTE has been shown to exhibit good performances when combined to standard classification algorithms (see, e.g., Mohammed et al., 2020). However, there exist only few works that aim at understanding theoretically SMOTE behavior. In this section, we assume that X_1, \dots, X_n are i.i.d samples from the minority class (that is, $Y_i = 1$ for all $i \in [n]$), with a common density f_X with bounded support, denoted by \mathcal{X} .

Lemma 3.1 (Convexity). *Given f_X the distribution density of the minority class, with support \mathcal{X} , for all K, n , the associated SMOTE density $f_{Z_{K,n}}$ satisfies*

$$\text{Supp}(f_{Z_{K,n}}) \subseteq \text{Conv}(\mathcal{X}). \quad (1)$$

By construction, synthetic observations generated by SMOTE cannot fall outside the convex hull of \mathcal{X} . Equation equation 1 is not an equality, as SMOTE samples are the convex combination of only two original samples. For example, in dimension two, if \mathcal{X} is concentrated near the vertices of a triangle, then SMOTE samples are distributed near the triangle edges, whereas $\text{Conv}(\mathcal{X})$ is the surface delimited by the triangle.

SMOTE algorithm has only one hyperparameter K , which is the number of nearest neighbors taken into account for building the linear interpolation. By default, this parameter is set to 5. The following theorem describes the behavior of SMOTE distribution asymptotically, as $K/n \rightarrow 0$.

Theorem 3.2. *For all Borel sets $B \subset \mathbb{R}^d$, if $K/n \rightarrow 0$, as n tends to infinity, we have*

$$\lim_{n \rightarrow \infty} \mathbb{P}[Z_{K,n} \in B] = \mathbb{P}[X \in B]. \quad (2)$$

The proof of Theorem 3.2 can be found in B.2. Theorem 3.2 proves that the random variables $Z_{K,n}$ generated by SMOTE converge in distribution to the original random variable X , provided that K/n tends to zero. From a practical point of view, Theorem 3.2 guarantees asymptotically the ability of SMOTE to regenerate the distribution of the minority class. This highlights a good behavior of the default setting of SMOTE ($K = 5$), as it can create more data points, different from the original sample, and distributed as the original sample. Note that Theorem 3.2 is very generic, as it makes no assumptions on the distribution of X .

SMOTE distribution has been derived in Theorem 1 and Lemma 1 in Elreedy et al. (2023). We provide here a slightly different expression for the density of the data generated by SMOTE, denoted by $f_{Z_{K,n}}$. Although our proof shares the same structure as that of Elreedy et al. (2023), our starting point is different, as we consider random variables instead of geometrical arguments. The proof can be found in Section B.3. When no confusion is possible, we simply write f_Z instead of $f_{Z_{K,n}}$.

Lemma 3.3. *Let X_c be the central point chosen in a SMOTE iteration. Then, for all $x_c \in \mathcal{X}$, the random variable $Z_{K,n}$ generated by SMOTE has a conditional density $f_{Z_{K,n}}(\cdot | X_c = x_c)$ which satisfies*

$$f_{Z_{K,n}}(z | X_c = x_c) = (n - K - 1) \binom{n-1}{K} \int_0^1 \frac{1}{w^d} f_X \left(x_c + \frac{z - x_c}{w} \right) \times \mathcal{B}(n - K - 1, K; 1 - \beta_{x_c, z, w}) dw, \quad (3)$$

where $\beta_{x_c, z, w} = \mu_X(B(x_c, \|z - x_c\|/w))$ and μ_X is the probability measure associated to f_X . Using the following substitution $w = \|z - x_c\|/r$, we have,

$$f_{Z_{K,n}}(z | X_c = x_c) = (n - K - 1) \binom{n-1}{K} \int_{r=\|z-x_c\|}^{\infty} f_X \left(x_c + \frac{(z - x_c)r}{\|z - x_c\|} \right) \times \frac{r^{d-2} \mathcal{B}(n - K - 1, K; 1 - \mu_X(B(x_c, r)))}{\|z - x_c\|^{d-1}} dr. \quad (4)$$

A close inspection of Lemma 3.3 allows us to derive more precise bounds about the behavior of SMOTE, as established in Theorem 3.5.

Assumption 3.4. There exists $R > 0$ such that $\mathcal{X} \subset B(0, R)$. Besides, there exist $0 < C_1 < C_2 < \infty$ such that for all $x \in \mathbb{R}^d$, $C_1 \mathbb{1}_{x \in \mathcal{X}} \leq f_X(x) \leq C_2 \mathbb{1}_{x \in \mathcal{X}}$.

Theorem 3.5. *Grant Assumption 3.4. Let $x_c \in \mathcal{X}$ and $\alpha \in (0, 2R)$. For all $K \leq (n - 1)\mu_X(B(x_c, \alpha))$, we have*

$$\mathbb{P}(\|Z_{K,n} - X_c\|_2 \geq \alpha | X_c = x_c) \leq \eta_{\alpha, R, d} \exp \left(-2(n - 1) \left(\mu_X(B(x_c, \alpha)) - \frac{K}{n - 1} \right)^2 \right) \quad (5)$$

with $\eta_{\alpha, R, d} = C_2 C_d R^d \times \begin{cases} \ln \left(\frac{2R}{\alpha} \right) & \text{if } d = 1, \\ \frac{1}{d-1} \left(\left(\frac{2R}{\alpha} \right)^{d-1} - 1 \right) & \text{if } d > 1. \end{cases}$

Consequently, if $\lim_{n \rightarrow \infty} K/n = 0$, we have, for all $x_c \in \mathcal{X}$, $Z_{K,n} | X_c = x_c \rightarrow x_c$ in probability.

The proof of Theorem 3.5 can be found in B.4. Theorem 3.5 establishes an upper bound on the distance between an observation generated by SMOTE and its central point. Asymptotically, when K/n tends to zero, the new synthetic observation concentrates around the central point. Recall that, by default, $K = 5$ in SMOTE algorithm. Therefore, Theorem 3.2 and Theorem 3.5 prove that, with the default settings, SMOTE asymptotically targets the original density of the minority class and generates new observations very close to the original ones. The following result establishes the characteristic distance between SMOTE observations and their central points.

Corollary 3.6. *Grant Assumption 3.4. For all $d \geq 2$, for all $\gamma \in (0, 1/d)$, we have*

$$\mathbb{P} [\|Z_{K,n} - X_c\|_2^2 > 12R(K/n)^\gamma] \leq \left(\frac{K}{n}\right)^{2/d-2\gamma}. \quad (6)$$

The proof of Corollary 3.6 can be found in B.5 and is an adaptation of Theorem 2.4 in Biau & Devroye (2015). The characteristic distance between a SMOTE observation and the associated central point is of order $(K/n)^{1/d}$. As expected from the curse of dimensionality, this distance increases with the dimension d . Choosing K that increases with n leads to larger characteristic distances: SMOTE observations are more distant from their central points. Corollary 3.6 leads us to choose K such that K/n does not tend too fast to zero, so that SMOTE observations are not too close to the original minority samples. However, choosing such a K can be problematic, especially near the boundary of the support, as shown in the following theorem.

Theorem 3.7. *Grant Assumption 3.4 with $\mathcal{X} = B(0, R)$. Let $\varepsilon \in (0, R)$ such that $(\frac{\varepsilon}{R})^{1/2} \leq \frac{c_d}{\sqrt{2d}C_2}$. Then, for all $1 \leq K < n$, and all $z \in B(0, R) \setminus B(0, R - \varepsilon)$, and for all $d > 1$, we have*

$$f_{Z_{K,n}}(z) \leq C_2^{3/2} \left(\frac{2^{d+2}c_d^{1/2}}{d^{1/2}}\right) \left(\frac{n-1}{K}\right) \left(\frac{\varepsilon}{R}\right)^{1/4}. \quad (7)$$

The proof of Theorem 3.7 can be found in B.6. Theorem 3.7 establishes an upper bound of SMOTE density at points distant from less than ε from the boundary of the minority class support. More precisely, Theorem 3.7 shows that SMOTE density vanishes as $\varepsilon^{1/4}$ near the boundary of the support. Choosing $\varepsilon/R = o((K/n)^4)$ leads to a vanishing upper bound, which proves that SMOTE density is unable to reproduce the original density $f_X \geq C_1$ in the peripheral area $B(0, R) \setminus B(0, R - \varepsilon)$. Such a behavior was expected since the boundary bias of local averaging methods (kernels, nearest neighbors, decision trees) has been extensively studied (see, e.g. Jones, 1993; Arya et al., 1995; Arlot & Genuer, 2014; Mourrada et al., 2020).

For default settings of SMOTE (i.e., $K = 5$), and large sample size, this area is relatively small ($\varepsilon = o(n^{-4})$). Still, Theorem 3.7 provides a theoretical ground for understanding the behavior of SMOTE near the boundary, a phenomenon that has led to introduce variants of SMOTE to circumvent this issue (see Borderline SMOTE in Han et al., 2005). While increasing K leads to more diversity in the generated observations (as shown in Theorem 3.5), it increases the boundary bias of SMOTE. Indeed, choosing $K = n^{3/4}$ implies a boundary effect in the peripheral area $B(0, R) \setminus B(0, R - \varepsilon)$ for $\varepsilon = o(1/n)$, which may not be negligible. Finally, note that constants in the upper bounds are of reasonable size. Letting $d = 3$, $K = 5$, $X \sim \mathcal{U}(B_d(0, 1))$, the upper bound turns into $0.89n\varepsilon^{1/4}$.

3.3 NUMERICAL ILLUSTRATIONS

Through Section 3, we highlighted the fact that SMOTE asymptotically regenerates the distribution of the minority class, by tending to copy the minority samples. The purpose of this section is to numerically illustrate the theoretical limitations of SMOTE, typically with the default value $K = 5$.

Simulated data In order to measure the similarity between any generated data set $\mathbf{Z} = \{Z_1, \dots, Z_m\}$ and the original data set $\mathbf{X} = \{X_1, \dots, X_n\}$, we compute $C(\mathbf{Z}, \mathbf{X}) = \frac{1}{m} \sum_{i=1}^m \|Z_i - X_{(1)}(Z_i)\|_2$, where $X_{(1)}(Z_i)$ is the nearest neighbor of Z_i among X_1, \dots, X_n . Intuitively, this quantity measures how far the generated data set is from the original observations: if the new data are copies of the original ones, this measure equals zero. We apply the following protocol: for each value of n ,

1. Generate \mathbf{X} composed of n i.i.d samples distributed as $\mathcal{U}([-3, 3]^2)$.

2. Generate \mathbf{Z} composed of $m = 1000$ new i.i.d observations by applying SMOTE procedure on the original data set \mathbf{X} , with different values of K . Compute $C(\mathbf{Z}, \mathbf{X})$.
3. Generate $\tilde{\mathbf{X}}$ composed of m i.i.d new samples distributed as $\mathcal{U}([-3, 3]^2)$. Compute $C(\tilde{\mathbf{X}}, \mathbf{X})$, which is a reference value in the ideal case of new points sampled from the same distribution.

Steps 1-3 are repeated 75 times. The average of $C(\mathbf{Z}, \mathbf{X})$ (resp. $C(\tilde{\mathbf{X}}, \mathbf{X})$) over these repetitions is computed and denoted by $\bar{C}(\mathbf{Z}, \mathbf{X})$ (resp. $\bar{C}(\tilde{\mathbf{X}}, \mathbf{X})$). We consider the metric $\bar{C}(\mathbf{Z}, \mathbf{X})/\bar{C}(\tilde{\mathbf{X}}, \mathbf{X})$, depicted in Figure 1 (see also Figure 3 in Appendix for $\bar{C}(\mathbf{Z}, \mathbf{X})$).

Results. Figure 1 shows the renormalized quantity $\bar{C}(\mathbf{Z}, \mathbf{X})/\bar{C}(\tilde{\mathbf{X}}, \mathbf{X})$ as a function of n . We notice that the asymptotic for $K = 5$ is different since it is the only one where the distance between SMOTE data points and original data points does not vary with n . Besides, this distance is smaller than the other ones, thus stressing out that the SMOTE data points are very close to the original distribution for $K = 5$. Note that, for the other asymptotics in K , the diversity of SMOTE observations increases with n , meaning $C(\mathbf{Z}, \mathbf{X})$ gets closer from $\bar{C}(\tilde{\mathbf{X}}, \mathbf{X})$. This behavior in terms of average distance is ideal, since $\tilde{\mathbf{X}}$ is drawn from the same theoretical distribution as \mathbf{X} . On the contrary, $K = 5$ keeps a lower average distance, showing a lack of diversity of generated points. Besides, this diversity is asymptotically more important for $K = 0.1n$ and $K = 0.01n$. This corroborates our theoretical findings (Theorem 3.2) as these asymptotics do not satisfy $K/n \rightarrow 0$. Indeed, when K is set to a fraction of n , the SMOTE distribution does not converge to the original distribution anymore, therefore generating data points that are not simple copies of the original uniform samples. By construction, SMOTE data points are close to central points, which may explain why the quantity of interest in Figure 1 is smaller than 1.

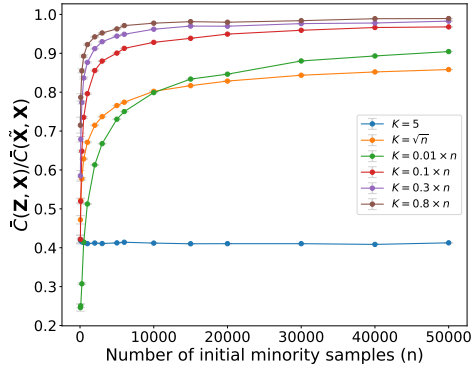


Figure 1: $\bar{C}(\mathbf{Z}, \mathbf{X})/\bar{C}(\tilde{\mathbf{X}}, \mathbf{X})$ with $\mathcal{U}([-3, 3]^2)$.

Extension to real-world data sets We extended our protocol to a real-world data set by splitting the data into two sets of equal size \mathbf{X} and $\tilde{\mathbf{X}}$. The first one is used for applying SMOTE strategies to sample \mathbf{Z} and the other set is used to compute the normalization factor $\bar{C}(\tilde{\mathbf{X}}, \mathbf{X})$. More details about this variant of the protocol are available on Appendix A.

Results We apply the adapted protocol to Phoneme data set, described in Table 1. Figure 2 displays the quantity $\bar{C}(\mathbf{Z}, \mathbf{X})/\bar{C}(\tilde{\mathbf{X}}, \mathbf{X})$ as a function of the size n of the minority class. As above, we observe in Figure 2 that the average normalized distance $\bar{C}(\mathbf{Z}, \mathbf{X})/\bar{C}(\tilde{\mathbf{X}}, \mathbf{X})$ increases for all strategies but the one with $K = 5$. The strategies using a value of hyperparameter K such that $K/n \rightarrow 0$ seem to converge to a value smaller than all the strategies with K such that $K/n \not\rightarrow 0$.

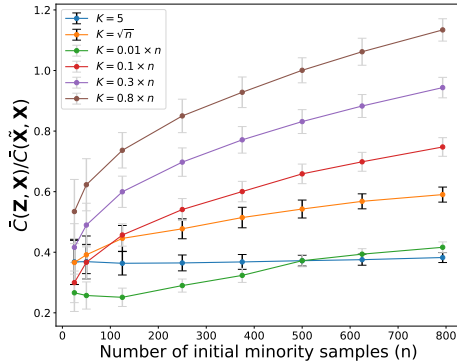


Figure 2: $\bar{C}(\mathbf{Z}, \mathbf{X})/\bar{C}(\tilde{\mathbf{X}}, \mathbf{X})$ with Phoneme data.

4 PREDICTIVE EVALUATION ON REAL-WORLD DATA SETS

In this section, we first describe the different rebalancing strategies and the two new ones we propose. Then, we describe our experimental protocol before discussing our results.

4.1 REBALANCING STRATEGIES

Class-weight (CW) [Model-level strategy] The class weighting strategy assigns the same weight (chosen as hyperparameter) to each minority samples. The default setting for this strategy is to choose a weight ρ such that $\rho n = N - n$, where n and $N - n$ are respectively the number of minority and majority samples in the data set.

Over/Under Sampling strategies [Non-synthetic data-level strategies] Random Under Sampling (RUS) acts on the majority class by selecting uniformly without replacement several samples in order to obtain a prespecified size for the majority class. Similarly, Random Over Sampling (ROS) acts on the minority class by selecting uniformly with replacement several samples to be copied in order to obtain a prespecified size for the minority class.

NearMissOne [Non-synthetic data-level strategy]

NearMissOne is an undersampling procedure. For each sample X_i in the majority class, the averaged distance of X_i to its K nearest neighbors in the minority class is computed. Then, the samples X_i are ordered according to this averaged distance. Finally, iteratively, the first X_i is dropped until the given number/ratio is reached. Consequently, the X_i with the smallest mean distance are dropped firstly.

Borderline SMOTE 1 and 2 [Synthetic data-level strategies]

Borderline SMOTE 1 (Han et al., 2005) procedure works as follows. For each individual X_i in the minority class, let $m_-(X_i)$ be the number of samples of the majority class among the m nearest neighbors of X_i , where m is a hyperparameter. For all X_i in the minority class such that $m/2 \leq m_-(X_i) < m$, generate q successive samples $Z = WX_i + (1 - W)X_k$ where $W \sim \mathcal{U}([0, 1])$ and X_k is selected among the K nearest-neighbors of X_i in the minority class. In Borderline SMOTE 2 (Han et al., 2005), the selected neighbor X_k is chosen from the neighbors of both positive and negative classes, and Z is sampled with $W \sim \mathcal{U}([0, 0.5])$.

The limitations of SMOTE highlighted in Section 3 drive us to two new rebalancing strategies.

CV SMOTE [Synthetic data-level strategy] We introduce a new algorithm, called CV SMOTE, that finds the best hyperparameter K among a prespecified grid via a 5-fold cross-validation procedure. The grid is composed of the set $\{1, 2, \dots, 15\}$ extended with the values $[0.01n_{train}]$, $[0.1n_{train}]$, $[0.5n_{train}]$, $[0.7n_{train}]$ and $[\sqrt{n_{train}}]$, where n_{train} is the number of minority samples in the training set. Recall that through Theorem 3.5, we show that SMOTE procedure with the default value $K = 5$ asymptotically copies the original samples. The idea of CV SMOTE is then to test several (larger) values of K in order to avoid duplicating samples, therefore improving predictive performances. CV SMOTE is one of the simplest ideas to solve some SMOTE limitations, which were highlighted theoretically in Section 3.

Multivariate Gaussian SMOTE(K) (MGS) [Synthetic data-level strategy] We introduce a new oversampling strategy in which new samples are generated from the distribution $\mathcal{N}(\hat{\mu}, \hat{\Sigma})$, where the empirical mean $\hat{\mu}$ and covariance matrix $\hat{\Sigma}$ are estimated using the K neighbors and the central point (see Algorithm 2 for details). By default, we choose $K = d + 1$, so that estimated covariance matrices can be of full rank. MGS produces more diverse synthetic observations than SMOTE as they are spread in all directions (in case of full-rank covariance matrix) around the central point. Besides, sampling from a normal distribution may generate points outside the convex hull of the nearest neighbors.

4.2 PRELIMINARY RESULTS

Initial data sets We employ classical tabular data sets already used in Grinsztajn et al. (2022). We also used some data sets from UCI Irvine (see Dua & Graff, 2017; Grinsztajn et al.,

Table 1: Initial data sets.

	N	n/N	d
Haberman	306	26%	3
Ionosphere	351	36%	32
Breast cancer	630	36%	9
Pima	768	35%	8
Vehicle	846	23%	18
Yeast	1 462	11%	8
Abalone	4 177	1%	8
Wine	4 974	4%	11
Phoneme	5 404	29%	5
MagicTel	13 376	50%	10
House_16H	22 784	30%	16
California	20 634	50%	8
CreditCard	284 315	0.2%	29

2022) and other public data sets such as Phoneme (Alinat, 1993) and Credit Card (Dal Pozzolo et al., 2015). All data sets are described in Table 1 and we call them *initial data sets*. As we want to compare several rebalancing methods including SMOTE, originally designed to handle continuous variables only, we have removed all categorical variables in each data set.

Protocol We compare the different rebalancing strategies on the initial data sets of Table 1. We employ a 5-fold stratified cross-validation, and apply each rebalancing strategy on four training folds, in order to obtain the same number of minority/majority samples. Then, we train a Random Forest classifier (showing good predictive performance, see Grinsztajn et al., 2022) on the same folds, and evaluate its performance on the remaining fold, via the ROC AUC. Results are averaged over the five test folds and over 20 repetitions of the cross-validation. We use the `RandomForestClassifier` module in *scikit-learn* (Pedregosa et al., 2011) and tune the tree depth (when desired) via nested cross-validation Cawley & Talbot (2010). We use the implementation of *imb-learn* (Lemaître et al., 2017) for the state-of-the-art rebalancing strategies (see Appendix A.2 for implementation details).

None is competitive for low imbalanced data sets For 10 initial data sets out of 13, applying no strategy is the best, probably highlighting that the imbalance ratio is not high enough or the learning task not difficult enough to require a tailored rebalancing strategy. Therefore, considering only continuous input variables, and measuring the predictive performance with ROC AUC, we observe that dedicated rebalancing strategies are not required for most data sets. While the performance without applying any strategy was already perceived in the literature (see, e.g., Han et al., 2005; He et al., 2008), we believe that our analysis advocates for its broad use in practice, at least as a default method. Note that for these 10 data sets, qualified as low imbalanced, applying no rebalancing strategy is on par with the CW strategy, one of the most common rebalancing strategies (regardless of tree depth tuning, see Table 5 and Table 7).

4.3 EXPERIMENTS ON HIGHLY IMBALANCED DATA SETS

Strengthening the imbalance To analyze what could happen for data sets with higher imbalance ratio, we subsample the minority class for each one of the initial data sets mentioned above, so that the resulting imbalance ratio is set to 20%, 10% or 1% (when possible, taking into account dimension d). By doing so, we reproduce the high imbalance that is often encountered in practice (see He & Garcia, 2009). We apply our subsampling strategy once for each data set and each imbalance ratio in a nested fashion, so that the minority samples of the 1% data set are included in the minority samples of the 10% data set. The new data sets thus obtained are called *subsampled data sets* and presented in Table 4 in Appendix A.2. For the sake of brevity, we display in Table 2 the data sets among the initial and subsampled for which the None strategy is not the best (up to its standard deviation). The others are presented in Table 5 in Appendix A.3.

Hereafter, we discuss the performances of rebalancing methods presented in Table 2. We remark that the included data sets correspond to the most imbalanced subsampling for each data set, or simply the initial data set in case of high initial imbalance. Therefore, in the following, we refer to them as *highly imbalanced data sets*.

Performances on highly imbalanced data sets Whilst in the vast majority of experiments, applying no rebalancing is among the best approaches to deal with imbalanced data (see Table 5), it seems to be outperformed by dedicated rebalancing strategies for highly imbalanced data sets (Table 2). Surprisingly, most rebalancing strategies do not benefit drastically from tree depth tuning, with the notable exceptions of applying no rebalancing and CW (see the differences between Table 2 and Table 6).

Algorithm 2 Multivariate Gaussian SMOTE iteration.

Input: Minority class samples X_1, \dots, X_n , number K of nearest-neighbors.

Select uniformly X_c among X_1, \dots, X_n .

Denote by I the set composed of the $K + 1$ nearest-neighbors of X_c among X_1, \dots, X_n including X_c (w.r.t. L_2 norm).

$$\hat{\mu} \leftarrow \frac{1}{K+1} \sum_{x \in I} x$$

$$\hat{\Sigma} \leftarrow \frac{1}{K+1} \sum_{x \in I} (x - \hat{\mu})^T (x - \hat{\mu})$$

Sample $Z \sim \mathcal{N}(\hat{\mu}, \hat{\Sigma})$

Return Z

Table 2: Highly imbalanced data sets ROC AUC (max_depth tuned with ROC AUC). Only data sets whose ROC AUC of at least one rebalancing strategy is larger than that of None strategy plus its standard deviation are displayed. Undersampled data sets are in italics. Standard deviations are displayed in Table 10.

Strategy	None	CW	RUS	ROS	Near Miss1	BS1	BS2	SMOTE	CV SMOTE	MGS ($d + 1$)
<i>CreditCard</i> (0.2%)	0.966	0.967	0.970	0.935	0.892	0.949	0.944	0.947	0.954	0.952
<i>Abalone</i> (1%)	0.764	0.748	0.735	0.722	0.656	0.744	0.753	0.741	0.791	0.802
<i>Phoneme</i> (1%)	0.897	0.868	0.868	0.858	0.698	0.867	0.869	0.888	0.924	0.915
<i>Yeast</i> (1%)	0.925	0.920	0.938	0.908	0.716	0.949	0.954	0.955	0.942	0.945
<i>Wine</i> (4%)	0.928	0.925	0.915	0.924	0.682	0.933	0.927	0.934	0.938	0.941
<i>Pima</i> (20%)	0.798	0.808	0.799	0.790	0.777	0.793	0.788	0.789	0.787	0.787
<i>Haberman</i> (10%)	0.708	0.709	0.720	0.704	0.697	0.723	0.721	0.719	0.742	0.744
<i>MagicTel</i> (20%)	0.917	0.921	0.917	0.922	0.649	0.920	0.905	0.921	0.919	0.913
<i>California</i> (1%)	0.887	0.877	0.880	0.883	0.630	0.885	0.874	0.906	0.916	0.923

Re-weighting strategies RUS, ROS and CW are similar strategies in that they are equivalent to applying weights to the original samples. When random forests with default parameters are applied, we see that ROS and CW have the same predictive performances (see Table 6). This was expected, as ROS assigns random weights to minority samples, whose expectation is that of the weights produced by CW. More importantly, RUS has better performances than both ROS and CW. This advocates for the use of RUS among these three rebalancing methods, as RUS produces smaller data sets, thus resulting in faster learning phases. We describe another benefit of RUS in the next paragraph.

Implicit regularization The good performances of RUS, compared to ROS and CW, may result from the implicit regularization of the maximum tree depth. Indeed, fewer samples are available after the undersampling step, which makes the resulting trees shallower, as by default, each leaf contains at least one observation. When the maximum tree depth is fixed, RUS, ROS and CW strategies have the same predictive performances (see Table 8 or Table 9). Similarly, when the tree depth is tuned, the predictive performances of RUS, ROS and CW are smoothed out (see Table 2). This highlights the importance of implicit regularization on RUS good performances.

SMOTE and CV-SMOTE Default SMOTE ($K = 5$) has a tendency to duplicate original observations, as shown by Theorem 3.5. This behavior is illustrated through our experiments when the tree depth is fixed. In this context, SMOTE ($K = 5$) has the same behavior as ROS, a method that copies original samples (see Table 8 or Table 9). When the tree depth is tuned, SMOTE may exhibit better performances compared to reweighting methods (ROS, RUS, CW), probably due to a higher tree depth. Indeed, even if synthetic data are close to the original samples, they are distinct and thus allow for more splits in the tree structure. However, as expected, CV SMOTE performances are higher than default SMOTE ($K = 5$) on most data sets (see Table 2).

MGS Our second new publicly available ³ strategy exhibits good predictive performances (best performance in 4 out of 9 data sets in Table 2). This could be explained by the Gaussian sampling of synthetic observations that allows generating data points outside the convex hull of the minority class, therefore limiting the border phenomenon, established in Theorem 3.7. Note that with MGS, there is no need of tuning the tree depth: predictive performances of default RF are on par with tuned RF. Thus, MGS is a promising new strategy.

4.4 SUPPLEMENTARY RESULTS

Logistic Regression When replacing random forests with Logistic regression in the above protocol (see Table 15), we still do not observe strong benefits of using a rebalancing strategies for most data sets. We compared in Table 17 the LDAM and Focal losses intended for long-tailed learning, using PyTorch. Table 17 shows that Focal loss performances are on par with the None strategy ones, while the performances of LDAM are significantly lower. Such methods do not seem promising for binary classification on tabular data, for which they were not initially intended.

³https://github.com/anonymous8880/smote_study

LightGBM - ROC AUC We apply the same protocol as in Section 4.2, using LightGBM (a second-order boosting algorithm, see Ke et al., 2017) instead of random forests. Again, only data sets such that None strategy is not competitive (in terms of ROC AUC) are displayed in Table 3 (the remaining ones can be found in Table 20). In Table 3, we note that our introduced strategies, CV-SMOTE and MGS, display good predictive results.

Table 3: LightGBM ROC AUC. Only data sets whose ROC AUC of at least one rebalancing strategy is larger than that of None strategy plus its standard deviation are displayed. Undersampled data sets are in italics. Standard deviations are displayed in Table 20.

Strategy	None	CW	RUS	ROS	Near Miss1	BS1	BS2	SMOTE	CV SMOTE	MGS ($d + 1$)
<i>CreditCard</i> (0.2%)	0.761	0.938	0.970	0.921	0.879	0.941	0.932	0.937	0.950	0.956
<i>Abalone</i> (1%)	0.738	0.738	0.726	0.738	0.700	0.750	0.757	0.748	0.775	0.745
<i>Haberman</i> (10%)	0.691	0.689	0.575	0.643	0.564	0.710	0.674	0.712	0.726	0.729
<i>House_16H</i> (1%)	0.903	0.896	0.899	0.896	0.605	0.907	0.909	0.894	0.894	0.912

PR AUC As above, we apply exactly the same protocol as described in Section 4.2 using the PR AUC metric instead of the ROC AUC. The results are displayed in Table 13 and Table 14 for tuned random forests. For LightGBM classifiers, results are available in Table 18 and Table 19. Again, we only focus on data sets such that None strategy is not competitive (in terms of PR AUC). In Table 13, for random forests tuned on PR AUC, we remark that CV-SMOTE exhibits good performances, being among the best rebalancing strategy for 3 out of 4 data sets. For LightGBM classifier, in Table 18, we note that our introduced strategies, CV-SMOTE and MGS, display good predictive results.

5 CONCLUSION AND PERSPECTIVES

In this paper, we analyzed the impact of rebalancing strategies on predictive performance for binary classification tasks on tabular data. First, we prove that default SMOTE tends to copy the original minority samples asymptotically, and exhibits boundary artifacts, thus justifying several SMOTE variants. From a computational perspective, we show that applying no rebalancing is competitive for most datasets, when used in conjunction with a tuned random forest/Logistic regression/LightGBM, whether considering the ROC AUC or PR AUC as metric. For highly imbalanced data sets, rebalancing strategies lead to improved predictive performances, with or without tuning the maximum tree depth. The SMOTE variants we propose, CV-SMOTE and MGS, appear promising, with good predictive performances regardless of the hyperparameter tuning of random forests. Besides, our analysis sheds some lights on the performances of reweighting strategies (ROS, RUS, CW) and an implicit regularization phenomenon occurring when such rebalancing methods are used with random forests.

More analyses need to be carried out in order to understand the influence of MGS parameters (regularization of the covariance matrices, number of nearest neighbors...). We also plan to extend our new MGS method to handle categorical features, and compare the different rebalancing strategies in presence of continuous and categorical input variables.

REFERENCES

- 540
541
542 Anass Aghbalou, Anne Sabourin, and François Portier. Sharp error bounds for imbalanced classi-
543 fication: how many examples in the minority class? In *International Conference on Artificial*
544 *Intelligence and Statistics*, pp. 838–846. PMLR, 2024.
- 545 Gabriel Aguiar, Bartosz Krawczyk, and Alberto Cano. A survey on learning from imbalanced
546 data streams: taxonomy, challenges, empirical study, and reproducible experimental framework.
547 *Machine learning*, pp. 1–79, 2023.
- 548
549 Pierre Alinat. Periodic progress report 4, roars project esprit ii-number 5516. *Technical Thomson*
550 *Report TS ASM 93/S/EGS/NC*, 79, 1993.
- 551 Sylvain Arlot and Robin Genuer. Analysis of purely random forests bias. *arXiv preprint*
552 *arXiv:1407.3939*, 2014.
- 553
554 Sunil Arya, David M Mount, and Onuttom Narayan. Accounting for boundary effects in nearest
555 neighbor searching. In *Proceedings of the eleventh annual symposium on computational geome-*
556 *try*, pp. 336–344, 1995.
- 557 Thomas Benjamin Berrett. Modern k-nearest neighbour methods in entropy estimation, indepen-
558 dence testing and classification. 2017. doi: 10.17863/CAM.13756. URL [https://www.](https://www.repository.cam.ac.uk/handle/1810/267832)
559 [repository.cam.ac.uk/handle/1810/267832](https://www.repository.cam.ac.uk/handle/1810/267832).
- 560
561 Gérard Biau and Luc Devroye. *Lectures on the nearest neighbor method*, volume 246. Springer,
562 2015.
- 563 Chumphol Bunkhumpornpat, Krung Sinapiromsaran, and Chidchanok Lursinsap. Dbsmote:
564 density-based synthetic minority over-sampling technique. *Applied Intelligence*, 36:664–684,
565 2012.
- 566
567 Kaidi Cao, Colin Wei, Adrien Gaidon, Nikos Arechiga, and Tengyu Ma. Learning imbalanced
568 datasets with label-distribution-aware margin loss. *Advances in neural information processing*
569 *systems*, 32, 2019.
- 570 Gavin C Cawley and Nicola LC Talbot. On over-fitting in model selection and subsequent selection
571 bias in performance evaluation. *The Journal of Machine Learning Research*, 11:2079–2107, 2010.
- 572
573 Kamalika Chaudhuri, Kartik Ahuja, Martin Arjovsky, and David Lopez-Paz. Why does throwing
574 away data improve worst-group error? In *International Conference on Machine Learning*, pp.
575 4144–4188. PMLR, 2023.
- 576 Nitesh V Chawla, Kevin W Bowyer, Lawrence O Hall, and W Philip Kegelmeyer. Smote: synthetic
577 minority over-sampling technique. *Journal of artificial intelligence research*, 16:321–357, 2002.
- 578
579 Nitesh V Chawla, Aleksandar Lazarevic, Lawrence O Hall, and Kevin W Bowyer. Smoteboost:
580 Improving prediction of the minority class in boosting. In *Knowledge Discovery in Databases:*
581 *PKDD 2003: 7th European Conference on Principles and Practice of Knowledge Discovery in*
582 *Databases, Cavtat-Dubrovnik, Croatia, September 22-26, 2003. Proceedings 7*, pp. 107–119.
583 Springer, 2003.
- 584 Nitesh V Chawla, Nathalie Japkowicz, and Aleksander Kotcz. Special issue on learning from im-
585 balanced data sets. *ACM SIGKDD explorations newsletter*, 6(1):1–6, 2004.
- 586
587 Andrea Dal Pozzolo, Olivier Caelen, Reid A Johnson, and Gianluca Bontempi. Calibrating prob-
588 ability with undersampling for unbalanced classification. In *2015 IEEE symposium series on*
589 *computational intelligence*, pp. 159–166. IEEE, 2015.
- 590 Dheeru Dua and Casey Graff. Uci machine learning repository, 2017. URL [http://archive.](http://archive.ics.uci.edu/ml)
591 [ics.uci.edu/ml](http://archive.ics.uci.edu/ml).
- 592
593 Dina Elreedy and Amir F Atiya. A comprehensive analysis of synthetic minority oversampling
technique (smote) for handling class imbalance. *Information Sciences*, 505:32–64, 2019.

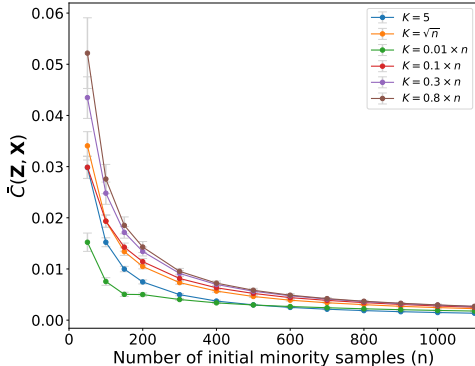
- 594 Dina Elreedy, Amir F. Atiya, and Firuz Kamalov. A theoretical distribution analysis of synthetic
595 minority oversampling technique (SMOTE) for imbalanced learning. *Machine Learning*, January
596 2023. ISSN 1573-0565. doi: 10.1007/s10994-022-06296-4. URL <https://doi.org/10.1007/s10994-022-06296-4>.
597
- 598 Léo Grinsztajn, Edouard Oyallon, and Gaël Varoquaux. Why do tree-based models still outperform
599 deep learning on typical tabular data? *Advances in neural information processing systems*, 35:
600 507–520, 2022.
601
- 602 Hui Han, Wen-Yuan Wang, and Bing-Huan Mao. Borderline-smote: a new over-sampling method in
603 imbalanced data sets learning. In *International conference on intelligent computing*, pp. 878–887.
604 Springer, 2005.
605
- 606 Charles R. Harris, K. Jarrod Millman, Stéfan J. van der Walt, Ralf Gommers, Pauli Virtanen,
607 David Cournapeau, Eric Wieser, Julian Taylor, Sebastian Berg, Nathaniel J. Smith, Robert
608 Kern, Matti Picus, Stephan Hoyer, Marten H. van Kerkwijk, Matthew Brett, Allan Haldane,
609 Jaime Fernández del Río, Mark Wiebe, Pearu Peterson, Pierre Gérard-Marchant, Kevin Sheppard,
610 Tyler Reddy, Warren Weckesser, Hameer Abbasi, Christoph Gohlke, and Travis E. Oliphant. Ar-
611 ray programming with NumPy. *Nature*, 585(7825):357–362, September 2020. doi: 10.1038/
612 s41586-020-2649-2. URL <https://doi.org/10.1038/s41586-020-2649-2>.
- 613 Amira Kamil Ibrahim Hassan and Ajith Abraham. Modeling insurance fraud detection using imbal-
614 anced data classification. In *Advances in Nature and Biologically Inspired Computing: Proceed-
615 ings of the 7th World Congress on Nature and Biologically Inspired Computing (NaBIC2015) in
616 Pietermaritzburg, South Africa, held December 01-03, 2015*, pp. 117–127. Springer, 2016.
617
- 618 Haibo He and Eduardo A Garcia. Learning from imbalanced data. *IEEE Transactions on knowledge
619 and data engineering*, 21(9):1263–1284, 2009.
- 620 Haibo He, Yang Bai, Eduardo A Garcia, and Shutao Li. Adasyn: Adaptive synthetic sampling ap-
621 proach for imbalanced learning. In *2008 IEEE international joint conference on neural networks
622 (IEEE world congress on computational intelligence)*, pp. 1322–1328. Ieee, 2008.
623
- 624 Jyoti Islam and Yanqing Zhang. Gan-based synthetic brain pet image generation. *Brain informatics*,
625 7:1–12, 2020.
- 626 M Chris Jones. Simple boundary correction for kernel density estimation. *Statistics and computing*,
627 3:135–146, 1993.
628
- 629 Firuz Kamalov, Amir F Atiya, and Dina Elreedy. Partial resampling of imbalanced data. *arXiv
630 preprint arXiv:2207.04631*, 2022.
631
- 632 Guolin Ke, Qi Meng, Thomas Finley, Taifeng Wang, Wei Chen, Weidong Ma, Qiwei Ye, and Tie-
633 Yan Liu. Lightgbm: A highly efficient gradient boosting decision tree. *Advances in neural
634 information processing systems*, 30, 2017.
- 635 Mohammed Khalilia, Sounak Chakraborty, and Mihail Popescu. Predicting disease risks from highly
636 imbalanced data using random forest. *BMC medical informatics and decision making*, 11:1–13,
637 2011.
638
- 639 Bartosz Krawczyk. Learning from imbalanced data: open challenges and future directions. *Progress
640 in Artificial Intelligence*, 5(4):221–232, 2016.
- 641 Guillaume Lemaître, Fernando Nogueira, and Christos K. Aridas. Imbalanced-learn: A python
642 toolbox to tackle the curse of imbalanced datasets in machine learning. *Journal of Machine
643 Learning Research*, 18(17):1–5, 2017. URL <http://jmlr.org/papers/v18/16-365.html>.
644
- 645
646
647 Tsung-Yi Lin, Priya Goyal, Ross Girshick, Kaiming He, and Piotr Dollár. Focal loss for dense
object detection. In *Proceedings of the IEEE international conference on computer vision*, pp.
2980–2988, 2017.

- 648 Inderjeet Mani and I Zhang. knn approach to unbalanced data distributions: a case study involv-
649 ing information extraction. In *Proceedings of workshop on learning from imbalanced datasets*,
650 volume 126, pp. 1–7. ICML, 2003.
- 651
- 652 Giovanna Menardi and Nicola Torelli. Training and assessing classification rules with imbalanced
653 data. *Data mining and knowledge discovery*, 28:92–122, 2014.
- 654
- 655 Ahmed Jameel Mohammed, Masoud Muhammed Hassan, and Dler Hussein Kadir. Improving clas-
656 sification performance for a novel imbalanced medical dataset using smote method. *International*
657 *Journal of Advanced Trends in Computer Science and Engineering*, 9(3):3161–3172, 2020.
- 658
- 659 Jaouad Mourtada, Stéphane Gaïffas, and Erwan Scornet. Minimax optimal rates for mondrian trees
660 and forests. *Annals of Statistics*, 48(4):2253–2276, 2020.
- 661
- 662 Hien M Nguyen, Eric W Cooper, and Katsuari Kamei. Borderline over-sampling for imbalanced
663 data classification. *International Journal of Knowledge Engineering and Soft Data Paradigms*, 3
664 (1):4–21, 2011.
- 665
- 666 Nam N Nguyen and Anh T Duong. Comparison of two main approaches for handling imbalanced
667 data in churn prediction problem. *Journal of advances in information technology*, 12(1), 2021.
- 668
- 669 Tingting Pan, Junhong Zhao, Wei Wu, and Jie Yang. Learning imbalanced datasets based on smote
670 and gaussian distribution. *Information Sciences*, 512:1214–1233, 2020.
- 671
- 672 Fabian Pedregosa, Gaël Varoquaux, Alexandre Gramfort, Vincent Michel, Bertrand Thirion, Olivier
673 Grisel, Mathieu Blondel, Peter Prettenhofer, Ron Weiss, Vincent Dubourg, et al. Scikit-learn:
674 Machine learning in python. *the Journal of machine Learning research*, 12:2825–2830, 2011.
- 675
- 676 Duraisamy Ramyachitra and Parasuraman Manikandan. Imbalanced dataset classification and solu-
677 tions: a review. *International Journal of Computing and Business Research (IJCBR)*, 5(4):1–29,
678 2014.
- 679
- 680 Ravid Shwartz-Ziv and Amitai Armon. Tabular data: Deep learning is not all you need. *Information*
681 *Fusion*, 81:84–90, 2022.
- 682
- 683 George Proctor Wadsworth, Joseph G Bryan, and A Cemal Eringen. Introduction to probability and
684 random variables. *Journal of Applied Mechanics*, 28(2):319, 1961.
- 685
- 686 Byron C Wallace and Issa J Dahabreh. Improving class probability estimates for imbalanced data.
687 *Knowledge and information systems*, 41(1):33–52, 2014.
- 688
- 689 Tarid Wongvorachan, Surina He, and Okan Bulut. A comparison of undersampling, oversampling,
690 and smote methods for dealing with imbalanced classification in educational data mining. *Inform-*
691 *ation*, 14(1):54, 2023.
- 692
- 693 Yuxi Xie, Min Qiu, Haibo Zhang, Lizhi Peng, and Zhenxiang Chen. Gaussian distribution based
694 oversampling for imbalanced data classification. *IEEE Transactions on Knowledge and Data*
695 *Engineering*, 34(2):667–679, 2020.
- 696
- 697 Ziyu Xu, Chen Dan, Justin Khim, and Pradeep Ravikumar. Class-weighted classification: Trade-
698 offs and robust approaches. In *International Conference on Machine Learning*, pp. 10544–10554.
699 PMLR, 2020.
- 700
- 701 Yifan Zhang, Bingyi Kang, Bryan Hooi, Shuicheng Yan, and Jiashi Feng. Deep long-tailed learning:
A survey. *IEEE Transactions on Pattern Analysis and Machine Intelligence*, 2023.
- Min Zhu, Jing Xia, Xiaoqing Jin, Molei Yan, Guolong Cai, Jing Yan, and Gangmin Ning. Class
weights random forest algorithm for processing class imbalanced medical data. *IEEE Access*, 6:
4641–4652, 2018.

702 A EXPERIMENTS

703
704 **Hardware** For all the numerical experiments, we use the following processor : AMD Ryzen
705 Threadripper PRO 5955WX: 16 cores, 4.0 GHz, 64 MB cache, PCIe 4.0. We also add access to
706 250GB of RAM.

707 A.1 NUMERICAL ILLUSTRATIONS



711
712
713
714
715
716
717
718
719
720
721
722
723
724
725
726
727
728
729
730
731
732
733
734
735
736
737
738
739
740
741
742
743
744
745
746
747
748
749
750
751
752
753
754
755

Figure 3: Average distance $\bar{C}(\mathbf{Z}, \mathbf{X})$.

Results with $\bar{C}(\mathbf{Z}, \mathbf{X})$ Figure 3 depicts the quantity $\bar{C}(\mathbf{Z}, \mathbf{X})$ as a function of the size of the minority class, for different values of K . The metric $\bar{C}(\mathbf{Z}, \mathbf{X})$ is consistently smaller for $K = 5$ than for other values of K , therefore highlighting that data generated by SMOTE with $K = 5$ are closer to the original data sample. This phenomenon is strengthened as n increases. This is an artifact of the simulation setting as the original data samples fill the input space as n increases.

More details on the numerical illustrations protocol applied to real-world data sets We apply SMOTE on real-world data and compare the distribution of the generated data points to the original distribution, using the metric $\bar{C}(\mathbf{Z}, \mathbf{X})/\bar{C}(\tilde{\mathbf{X}}, \mathbf{X})$.

For each value of n , we subsample n data points from the minority class. Then,

1. We uniformly split the data set into $X_1, \dots, X_{n/2}$ (denoted by \mathbf{X}) and $\tilde{X}_1, \dots, \tilde{X}_{n/2}$ (denoted by $\tilde{\mathbf{X}}$).
2. We generate a data set \mathbf{Z} composed of $m = n/2$ i.i.d new observations Z_1, \dots, Z_m by applying SMOTE procedure on the original data set \mathbf{X} , with different values of K . We compute $\bar{C}(\mathbf{Z}, \mathbf{X})$.
3. We use $\tilde{\mathbf{X}}$ in order to compute $\bar{C}(\tilde{\mathbf{X}}, \mathbf{X})$.

This procedure is repeated $B = 100$ times to compute averages values as in Section 3.3.

748 A.2 BINARY CLASSIFICATION PROTOCOL

General comment on the protocol For each data set, the ratio hyperparameters of each rebalancing strategy are chosen so that the minority and majority class have the same weights in the training phase. The main purpose is to apply the strategies exactly on the same data points (X_{train}), then train the chosen classifier and evaluate the strategies on the same X_{test} . This objective is achieved by selecting each time 4 fold for the training, apply each of the strategies to these 4 exact same fold.

The state-of-the-art rebalancing strategies (see Lemaître et al., 2017) are used with their default hyperparameter values.

Table 4: Subsampled data sets.

	N	n/N	d
<i>Haberman</i> (10%)	250	10%	3
<i>Ionosphere</i> (20%)	281	20%	32
<i>Ionosphere</i> (10%)	250	10%	32
<i>Breast cancer</i> (20%)	500	20%	9
<i>Breast cancer</i> (10%)	444	10%	9
Pima (20%)	625	20%	8
<i>Vehicle</i> (10%)	718	10%	18
<i>Yeast</i> (1%)	1 334	1%	8
<i>Phoneme</i> (20%)	4 772	20%	5
<i>Phoneme</i> (10%)	4 242	10%	5
<i>Phoneme</i> (1%)	3 856	1%	5
<i>MagicTel</i> (20%)	8 360	20%	10
<i>House_16H</i> (20%)	20 050	20%	16
<i>House_16H</i> (10%)	17 822	10%	16
<i>House_16H</i> (1%)	16 202	1%	16
<i>California</i> (20%)	12 896	20%	8
<i>California</i> (10%)	11 463	10%	8
<i>California</i> (1%)	10 421	1%	8

The subsampled data sets (see Table 4) can be obtained through the repository (the functions and the seeds are given in a jupyter notebook). For the CreditCard data set, a Time Series split is performed instead of a Stratified 5-fold, because of the temporality of the data. Furthermore, a group out is applied on the different scope time value.

For MagicTel and California data sets, the initial data sets are already balanced, leading to no opportunity for applying a rebalancing strategy. This is the reason why we do not include these original data sets in our study but only their subsampled associated data sets.

The `max_depth` hyperparameter is tuned using GridSearch function from scikit-learn. The grids minimum is 5 and the grid maximum is the mean depth of the given strategy for the given data set (when random forest is used without tuning depth hyperparameter). Then, using numpy (Harris et al., 2020), a list of integer of size 8 between the minimum value and the maximum is value is built. Finally, the "None" value is added to this list.

Mean standard deviation For each protocol run, we computed the standard deviation of the ROC AUC over the 5-fold. Then, all of these 100 standard deviation are averaged in order to get what we call in some of our tables the mean standard deviations. On Table 10, Table 11 and Table 17 means standard deviation over 100 runs are displayed for each strategy (no averaging is performed).

CV SMOTE We also apply our protocol for SMOTE with values of hyperparameter K depending on the number of minority inside the training set. The results are shown on both Table 12 and Table 16. As expected, CV SMOTE is most of the time the best strategy among the SMOTE variants for highly imbalanced data sets. This another illustration of our Theorem 3.5.

More results about None strategy from seminal papers Several seminal papers already noticed that the None strategy was competitive in terms of predictive performances. He et al. (2008) compare the None strategy, ADASYN and SMOTE, followed by a decision tree classifier on 5 data sets (including Vehicle, Pima, Ionosphere and Abalone). In terms of Precision and F1 score, the None strategy is on par with the two other rebalancing methods. Han et al. (2005) study the impact of Borderline SMOTE and others SMOTE variant on 4 data sets (including Pima and Haberman). The None strategy is competitive (in terms of F1 score) on two of these data sets.

Random forests - PR AUC We apply exactly the same protocol as described in Section 4.2 but using the PR AUC metric instead of the ROC AUC. Data sets such that the None strategy is not competitive (in terms of PR AUC) are displayed in Table 13, others can be found in Table 14. As

810 for the ROC AUC metric, None and CW strategies are competitive for a large number of data sets
811 (see Table 14). Furthermore, in Table 13, CV-SMOTE exhibits good performances, being among
812 the best rebalancing strategy for 3 out of 4 data sets.
813

814 **LightGBM - PR AUC** As above, we apply the same protocol as in Section 4.2, using the PR AUC
815 metric instead of the ROC AUC and LightGBM (a second-order boosting algorithm, see Ke et al.,
816 2017) instead of random forests. Again, only data sets such that None strategy is not competitive
817 (in terms of PR AUC) are displayed in Table 18 (the remaining ones can be found in Table 19).
818 In Table 18, we note that our introduced strategies, CV-SMOTE and MGS, display good predictive
819 results.

820 The classification experiments needed 2 months of calculation time.
821

822 A.3 ADDITIONAL EXPERIMENTS 823

824 **Tables** The tables in appendix can be divided into 3 categories. First, we have the tables related
825 to random forests. Then the tables related to logistic regression. Finally, we have the tables of
826 LightGBM classifiers. Here are some details fore each group:
827

- 828 • **Random Forest:** In Table 5, ROC AUC of the data sets not presented Table 2 are displayed
829 (using tuned forest on ROC AUC for both). In Table 6 and Table 7, ROC AUC of default
830 random forests are displayed for all the data sets. In Table 8 and Table 9 are displayed
831 default random forests ROC AUC with a max tree depth fixed to respectively 5 and the
832 value of RUS depth. Table 10 and Table 11 illustrate respectively the same setting as
833 Table 2 and Table 5 with the standard deviation displayed. In Table 12, the ROC AUC
834 of several SMOTE strategies with various K hyperparameter value are displayed using
835 defaults random forests for all data sets. PR AUC of tuned random forests on PR AUC are
836 displayed in Table 13 and Table 14.
- 837 • **Logistic Regression:** Table 15 display ROC AUC of several rebalancing strategies when
838 using Logistic regression. In Table 16, the ROC AUC of several SMOTE strategies with
839 various K hyperparameter value are displayed using logistic regression for all data sets.
840 Table 17 shows ROC AUC of None, LDAM and Focal loss strategies when using a logistic
841 regression reimplemented using PyTorch.
- 842 • **LightGBM:** The PR AUC and ROC AUC of the remaining data sets when using Light-
843 GBM classifiers are displayed respectively in Table 18/Table 19 and Table 20.
844
845
846
847
848
849
850
851
852
853
854
855
856
857
858
859
860
861
862
863

Table 5: Remaining data sets (without those of Table 2). Random Forest (max_depth= tuned with ROC AUC) ROC AUC for different rebalancing strategies and different data sets. Other data sets are presented in Table 2. The best strategy is highlighted in bold for each data set. Standard deviations are available on Table 11.

Strategy	None	CW	RUS	ROS	Near Miss1	BS1	BS2	SMOTE	CV SMOTE	MGS ($d + 1$)
Phoneme	0.962	0.961	0.951	0.962	0.910	0.960	0.961	0.962	0.961	0.959
<i>Phoneme</i> (20%)	0.952	0.952	0.935	0.953	0.793	0.950	0.951	0.953	0.953	0.949
<i>Phoneme</i> (10%)	0.936	0.935	0.909	0.936	0.664	0.933	0.932	0.935	0.938	0.932
Pima	0.833	0.832	0.828	0.823	0.817	0.814	0.811	0.820	0.824	0.826
Yeast	0.968	0.971	0.971	0.968	0.921	0.964	0.965	0.968	0.969	0.968
Haberman	0.686	0.686	0.685	0.673	0.686	0.682	0.670	0.681	0.690	0.698
<i>California</i> (20%)	0.956	0.955	0.951	0.956	0.850	0.953	0.947	0.955	0.956	0.954
<i>California</i> (10%)	0.948	0.946	0.940	0.948	0.775	0.945	0.934	0.947	0.950	0.948
House_16H	0.950	0.950	0.948	0.950	0.899	0.945	0.942	0.948	0.949	0.948
<i>House_16H</i> (20%)	0.950	0.949	0.946	0.949	0.835	0.943	0.938	0.946	0.947	0.946
<i>House_16H</i> (10%)	0.945	0.943	0.940	0.944	0.717	0.939	0.931	0.939	0.942	0.937
<i>House_16H</i> (1%)	0.906	0.893	0.902	0.885	0.600	0.894	0.896	0.898	0.905	0.889
Vehicle	0.995	0.994	0.990	0.994	0.978	0.994	0.993	0.994	0.995	0.995
Vehicle (10%)	0.992	0.991	0.982	0.989	0.863	0.991	0.989	0.992	0.993	0.994
Ionosphere	0.978	0.978	0.974	0.978	0.945	0.978	0.978	0.978	0.977	0.976
<i>Ionosphere</i> (20%)	0.988	0.986	0.974	0.987	0.881	0.981	0.974	0.981	0.983	0.983
<i>Ionosphere</i> (10%)	0.988	0.983	0.944	0.981	0.822	0.972	0.962	0.966	0.967	0.968
Breast Cancer	0.994	0.993	0.993	0.993	0.994	0.992	0.992	0.993	0.994	0.993
<i>Breast Cancer</i> (20%)	0.996	0.995	0.994	0.995	0.997	0.994	0.993	0.995	0.996	0.996
<i>Breast Cancer</i> (10%)	0.997	0.996	0.994	0.996	0.997	0.993	0.992	0.996	0.997	0.997

Table 6: Highly imbalanced data sets. Random Forest (max_depth= ∞) ROC AUC for different rebalancing strategies and different data sets. Data sets artificially undersampled for minority class are in italics. Other data sets are presented in Table 7. Mean standard deviations are computed.

Strategy	None	CW	RUS	ROS	Near Miss1	BS1	BS2	SMOTE	CV SMOTE	MGS ($d + 1$)
CreditCard (0.2%) (± 0.003)	0.930	0.927	0.968	0.932	0.887	0.933	0.941	0.950	0.961	0.953
Abalone (1%) (± 0.018)	0.716	0.698	0.732	0.699	0.652	0.745	0.754	0.744	0.777	0.805
<i>Phoneme</i> (1%) (± 0.020)	0.852	0.851	0.864	0.840	0.690	0.859	0.863	0.883	0.893	0.913
<i>Yeast</i> (1%) (± 0.020)	0.914	0.926	0.922	0.919	0.711	0.936	0.954	0.936	0.954	0.932
Wine (4%) (± 0.008)	0.926	0.923	0.917	0.927	0.693	0.934	0.927	0.934	0.935	0.939
<i>Pima</i> (20%) (± 0.009)	0.777	0.791	0.796	0.787	0.767	0.791	0.790	0.789	0.786	0.786
<i>Haberman</i> (10%) (± 0.028)	0.680	0.685	0.709	0.688	0.697	0.716	0.713	0.721	0.735	0.736
<i>MagicTel</i> (20%) (± 0.001)	0.917	0.921	0.917	0.921	0.650	0.920	0.905	0.921	0.921	0.913
<i>California</i> (1%) (± 0.009)	0.857	0.871	0.881	0.637	0.883	0.876	0.904	0.908	0.921	0.874

Table 7: Remaining data sets (without those of Table 2). Random Forest (max_depth= ∞) ROC AUC for different rebalancing strategies and different data sets. Only datasets such that the None strategy is on par with the best strategies are displayed. Other data sets are presented in Table 6. Mean standard deviations are computed. The best strategy is highlighted in bold for each data set.

Strategy	None	CW	RUS	ROS	Near Miss1	BS1	BS2	SMOTE	CV SMOTE	MGS ($d + 1$)
Phoneme (± 0.001)	0.961	0.962	0.951	0.963	0.909	0.961	0.961	0.962	0.961	0.959
Phoneme (20%)(± 0.002)	0.952	0.952	0.935	0.953	0.793	0.950	0.951	0.953	0.953	0.949
Phoneme (10%)(± 0.004)	0.937	0.936	0.911	0.937	0.668	0.933	0.932	0.935	0.915	0.933
Pima (± 0.005)	0.824	0.824	0.823	0.821	0.808	0.813	0.812	0.820	0.821	0.822
Yeast (± 0.003)	0.965	0.969	0.970	0.968	0.919	0.964	0.967	0.967	0.968	0.966
Haberman (± 0.017)	0.674	0.674	0.675	0.672	0.691	0.678	0.668	0.684	0.680	0.679
California (20%)(± 0.001)	0.956	0.955	0.951	0.956	0.850	0.954	0.947	0.955	0.954	0.954
California (10%)(± 0.001)	0.948	0.947	0.939	0.948	0.775	0.945	0.935	0.947	0.947	0.948
House_16H (± 0.001)	0.951	0.950	0.948	0.950	0.900	0.945	0.942	0.948	0.948	0.948
House_16H (20%)(± 0.001)	0.950	0.949	0.946	0.949	0.835	0.943	0.938	0.946	0.945	0.946
House_16H (10%)(± 0.001)	0.945	0.943	0.941	0.944	0.718	0.939	0.931	0.939	0.939	0.937
House_16H (1%)(± 0.001)	0.888	0.875	0.902	0.880	0.599	0.893	0.898	0.899	0.896	0.890
Vehicle (± 0.001)	0.995	0.994	0.990	0.995	0.977	0.994	0.994	0.994	0.994	0.995
Vehicle (10%)(± 0.003)	0.992	0.992	0.983	0.991	0.867	0.991	0.989	0.992	0.992	0.993
Ionosphere (± 0.003)	0.978	0.978	0.974	0.978	0.946	0.978	0.979	0.979	0.979	0.976
Ionosphere (20%)(± 0.004)	0.989	0.987	0.977	0.988	0.883	0.982	0.974	0.981	0.982	0.985
Ionosphere (10%)(± 0.008)	0.989	0.983	0.946	0.982	0.825	0.973	0.961	0.965	0.965	0.967
Breast Cancer (± 0.001)	0.994	0.993	0.993	0.993	0.994	0.992	0.992	0.993	0.993	0.993
Breast Cancer (20%)(± 0.001)	0.996	0.996	0.994	0.996	0.996	0.994	0.993	0.995	0.996	0.996
Breast Cancer (10%)(± 0.001)	0.997	0.996	0.994	0.996	0.997	0.994	0.993	0.996	0.996	0.997

Table 8: Highly imbalanced data sets. ROC AUC Random Forest with max_depth=5.

Strategy	None	CW	RUS	ROS	Near Miss1	BS1	BS2	SMOTE	CV SMOTE	MGS ($d + 1$)
CreditCard (0.2%)(± 0.002)	0.954	0.970	0.970	0.971	0.898	0.960	0.962	0.971	0.971	0.964
Abalone (1%)(± 0.017)	0.775	0.756	0.735	0.731	0.653	0.760	0.754	0.744	0.757	0.780
Phoneme (1%)(± 0.012)	0.891	0.871	0.870	0.867	0.697	0.865	0.851	0.882	0.878	0.886
Yeast (1%)(± 0.023)	0.923	0.921	0.934	0.887	0.709	0.933	0.922	0.945	0.940	0.944
Wine (4%)(± 0.005)	0.900	0.905	0.900	0.907	0.587	0.895	0.880	0.902	0.899	0.885
Pima (20%)(± 0.007)	0.802	0.811	0.805	0.809	0.778	0.804	0.805	0.805	0.806	0.804
Haberman (10%)(± 0.029)	0.714	0.722	0.708	0.723	0.699	0.749	0.738	0.751	0.750	0.759
MagicTel (20%)(± 0.001)	0.893	0.892	0.893	0.891	0.604	0.888	0.874	0.891	0.891	0.885
California (1%)(± 0.008)	0.880	0.877	0.875	0.874	0.631	0.852	0.838	0.867	0.866	0.878

Table 9: Highly imbalanced data sets. ROC AUC Random Forest with max_depth=RUS. On the last column, the value of maximal depth when using Random forest (max_depth= ∞) with RUS strategy for each data set.

Strategy	None	CW	RUS	ROS	Near Miss1	BS1	BS2	SMOTE	CV SMOTE	MGS ($d + 1$)	depth
CreditCard (0.2%)(± 0.002)	0.954	0.950	0.970	0.970	0.893	0.960	0.962	0.972	0.972	0.962	10
Abalone (1%)(± 0.017)	0.770	0.750	0.733	0.729	0.656	0.762	0.758	0.744	0.761	0.795	7
Phoneme (1%)(± 0.014)	0.897	0.874	0.872	0.869	0.695	0.869	0.858	0.887	0.880	0.894	6
Yeast (1%)(± 0.021)	0.928	0.927	0.928	0.893	0.725	0.924	0.919	0.934	0.925	0.945	3
Wine (4%)(± 0.006)	0.927	0.922	0.915	0.925	0.665	0.923	0.913	0.923	0.925	0.923	10
Pima (20%)(± 0.009)	0.784	0.797	0.793	0.790	0.768	0.792	0.789	0.792	0.792	0.790	10
Haberman (10%)(± 0.028)	0.696	0.711	0.713	0.721	0.690	0.737	0.729	0.740	0.748	0.752	7
MagicTel (20%)(± 0.001)	0.917	0.920	0.917	0.921	0.651	0.919	0.905	0.921	0.921	0.913	20
California (1%)(± 0.009)	0.895	0.871	0.877	0.875	0.639	0.876	0.859	0.884	0.903	0.913	10

Table 10: Table 2 with standard deviations over 100 runs. Random Forest (max_depth=tuned with ROC AUC) ROC AUC for different rebalancing strategies and different data sets. The best strategies are displayed in bold are displayed.

Strategy	None	CW	RUS	ROS	Near Miss1	BS1	BS2	SMOTE	CV SMOTE	MGS ($d + 1$)
CreditCard (0.2%)	0.966	0.967	0.970	0.935	0.892	0.949	0.944	0.947	0.954	0.952
std	± 0.003	± 0.003	± 0.003	± 0.003	± 0.005	± 0.005	± 0.006	± 0.004	± 0.003	± 0.003
Abalone (1%)	0.764	0.748	0.735	0.722	0.656	0.744	0.753	0.741	0.791	0.802
std	± 0.021	± 0.021	± 0.021	± 0.021	± 0.033	± 0.025	± 0.019	± 0.019	± 0.018	± 0.012
Phoneme (1%)	0.897	0.868	0.868	0.858	0.698	0.867	0.869	0.888	0.924	0.915
std	± 0.015	± 0.018	± 0.015	± 0.02	± 0.030	± 0.026	± 0.023	± 0.020	± 0.014	± 0.013
Yeast (1%)	0.925	0.920	0.938	0.908	0.716	0.949	0.954	0.955	0.942	0.945
std	± 0.017	± 0.030	± 0.026	± 0.021	± 0.069	± 0.0220	± 0.009	± 0.016	± 0.021	± 0.018
Wine (4%)	0.928	0.925	0.915	0.924	0.682	0.933	0.927	0.934	0.938	0.941
std	± 0.007	± 0.008	± 0.005	± 0.008	± 0.013	± 0.007	± 0.008	± 0.006	± 0.006	± 0.005
Pima (20%)	0.798	0.808	0.799	0.790	0.777	0.793	0.788	0.789	0.787	0.787
std	± 0.009	± 0.008	± 0.010	± 0.009	± 0.007	± 0.009	± 0.008	± 0.008	± 0.007	± 0.008
Haberman (10%)	0.708	0.709	0.720	0.704	0.697	0.723	0.721	0.719	0.742	0.744
std	± 0.027	± 0.029	± 0.040	± 0.024	± 0.038	± 0.027	± 0.027	± 0.024	± 0.022	± 0.026
MagicTel (20%)	0.917	0.921	0.917	0.922	0.649	0.920	0.905	0.921	0.919	0.913
std	± 0.001	± 0.001	± 0.001	± 0.001	± 0.005	± 0.001	± 0.002	± 0.001	± 0.001	± 0.001
California (1%)	0.887	0.877	0.880	0.883	0.630	0.885	0.874	0.906	0.916	0.923
std	± 0.010	± 0.013	± 0.010	± 0.011	± 0.012	± 0.014	± 0.013	± 0.011	± 0.007	± 0.006
House_16H (1%)	0.906	0.893	0.902	0.885	0.600	0.894	0.896	0.898	0.905	0.889
std	± 0.006	± 0.006	± 0.006	± 0.007	± 0.018	± 0.008	± 0.006	± 0.006	± 0.005	± 0.005

Table 11: Table 5 with standard deviations over 100 runs. Random Forest (max_depth=tuned with ROC AUC) ROC AUC for different rebalancing strategies and different data sets. The best strategies are displayed in bold.

Strategy	None	CW	RUS	ROS	Near Miss1	BS1	BS2	SMOTE	CV SMOTE	MGS ($d + 1$)
Phoneme	0.962	0.961	0.951	0.962	0.910	0.960	0.961	0.962	0.961	0.959
std	±0.001	±0.001	±0.001	±0.001	±0.003	±0.001	±0.001	±0.001	±0.001	±0.001
<i>Phoneme</i> (20%)	0.952	0.952	0.935	0.953	0.793	0.950	0.951	0.953	0.953	0.949
std	±0.001	±0.001	±0.002	±0.001	±0.014	±0.001	±0.001	±0.001	±0.001	±0.001
<i>Phoneme</i> (10%)	0.936	0.935	0.909	0.936	0.664	0.933	0.932	0.935	0.938	0.932
std	±0.003	±0.003	±0.005	±0.003	±0.013	±0.003	±0.004	±0.003	±0.003	±0.003
Pima	0.833	0.832	0.828	0.823	0.817	0.814	0.811	0.820	0.824	0.826
std	±0.004	±0.004	±0.004	±0.005	±0.004	±0.005	±0.005	±0.007	±0.006	±0.006
Yeast	0.968	0.971	0.971	0.968	0.921	0.964	0.965	0.968	0.969	0.968
std	±0.003	±0.002	±0.002	±0.004	±0.005	±0.004	±0.003	±0.004	±0.004	±0.003
Haberman	0.686	0.686	0.685	0.673	0.686	0.682	0.670	0.681	0.690	0.698
std	±0.020	±0.015	±0.025	±0.015	±0.012	±0.016	±0.014	±0.012	±0.015	±0.014
<i>California</i> (20%)	0.956	0.955	0.951	0.956	0.850	0.953	0.947	0.955	0.956	0.954
std	±0.001	±0.001	±0.001	±0.001	±0.002	±0.001	±0.001	±0.001	±0.001	±0.001
<i>California</i> (10%)	0.948	0.946	0.940	0.948	0.775	0.945	0.934	0.947	0.950	0.948
std	±0.002	±0.002	±0.002	±0.001	±0.004	±0.001	±0.002	±0.001	±0.001	±0.001
House_16H	0.950	0.950	0.948	0.950	0.899	0.945	0.942	0.948	0.949	0.948
std	±0.001	±0.001	±0.001	±0.001	±0.001	±0.001	±0.001	±0.001	±0.001	±0.001
<i>House_16H</i> (20%)	0.950	0.949	0.946	0.949	0.835	0.943	0.938	0.946	0.947	0.946
std	±0.001	±0.001	±0.001	±0.001	±0.001	±0.001	±0.001	±0.001	±0.001	±0.001
<i>House_16H</i> (10%)	0.945	0.943	0.940	0.944	0.717	0.939	0.931	0.939	0.942	0.937
std	±0.001	±0.001	±0.001	±0.001	±0.003	±0.001	±0.001	±0.001	±0.001	±0.001
<i>House_16H</i> (1%)	0.906	0.893	0.902	0.885	0.600	0.894	0.896	0.898	0.905	0.889
std	±0.006	±0.006	±0.006	±0.007	±0.018	±0.008	±0.006	±0.006	±0.005	±0.005
Vehicle	0.995	0.994	0.990	0.994	0.978	0.994	0.993	0.994	0.995	0.995
std	±0.001	±0.001	±0.001	±0.001	±0.003	±0.001	±0.001	±0.001	±0.001	±0.001
Vehicle (10%)	0.992	0.991	0.982	0.989	0.863	0.991	0.989	0.992	0.993	0.994
std	±0.002	±0.002	±0.005	±0.002	±0.010	±0.002	±0.003	±0.002	±0.001	±0.001
Ionosphere	0.978	0.978	0.974	0.978	0.945	0.978	0.978	0.978	0.977	0.976
std	±0.003	±0.003	±0.003	±0.003	±0.003	±0.003	±0.003	±0.003	±0.002	±0.002
<i>Ionosphere</i> (20%)	0.988	0.986	0.974	0.987	0.881	0.981	0.974	0.981	0.983	0.983
std	±0.002	±0.003	±0.005	±0.002	±0.013	±0.003	±0.004	±0.003	±0.004	±0.003
<i>Ionosphere</i> (10%)	0.988	0.983	0.944	0.981	0.822	0.972	0.962	0.966	0.967	0.968
std	±0.004	±0.005	±0.016	±0.005	±0.026	±0.007	±0.005	±0.005	±0.006	±0.006
Breast Cancer	0.994	0.993	0.993	0.993	0.994	0.992	0.992	0.993	0.994	0.993
std	±0.001	±0.001	±0.001	±0.001	±0.001	±0.001	±0.001	±0.001	±0.001	±0.001
<i>Breast Cancer</i> (20%)	0.996	0.995	0.994	0.995	0.997	0.994	0.993	0.995	0.996	0.996
std	±0.001	±0.001	±0.001	±0.001	±0.001	±0.002	±0.001	±0.001	±0.001	±0.001
<i>Breast Cancer</i> (10%)	0.997	0.996	0.994	0.996	0.997	0.993	0.992	0.996	0.997	0.997
std	±0.001	±0.001	±0.001	±0.001	±0.001	±0.001	±0.001	±0.001	±0.001	±0.001

1080
1081
1082
1083
1084
1085
1086
1087
1088
1089
1090
1091
1092
1093
1094
1095
1096
1097
1098
1099
1100
1101
1102
1103
1104
1105
1106
1107
1108
1109
1110
1111
1112
1113
1114
1115
1116
1117
1118
1119
1120
1121
1122
1123
1124
1125
1126
1127
1128
1129
1130
1131
1132
1133

Table 12: Highly imbalanced data sets at the top and remaining ones at the bottom. Random Forest (max_depth= ∞) ROC AUC. The best strategy is highlighted in bold for each data set.

SMOTE Strategy	$K = 5$	$K = \sqrt{n}$	$K = 0.01n$	$K = 0.1n$	CV SMOTE
CreditCard (± 0.004)	0.949	0.959	0.941	0.961	0.961
Abalone (1%)(± 0.021)	0.744	0.745	0.727	0.729	0.777
Phoneme (1%)(± 0.019)	0.883	0.880	0.872	0.871	0.893
Yeast (1%)(± 0.016)	0.940	0.935	0.932	0.931	0.954
Wine (4%)(± 0.006)	0.934	0.935	0.930	0.934	0.935
Pima (20%)(± 0.008)	0.789	0.786	0.790	0.788	0.786
Haberman (10%)(± 0.024)	0.721	0.723	0.715	0.725	0.735
MagicTel (20%)(± 0.001)	0.921	0.921	0.921	0.920	0.921
California (1%)(± 0.009)	0.904	0.905	0.893	0.905	0.908
Phoneme (± 0.001)	0.962	0.961	0.962	0.961	0.961
Phoneme (20%)(± 0.001)	0.953	0.952	0.953	0.952	0.953
Phoneme (10%)(± 0.003)	0.935	0.938	0.936	0.939	0.915
Pima (± 0.005)	0.820	0.819	0.821	0.819	0.821
Yeast (± 0.003)	0.967	0.970	0.968	0.969	0.968
Haberman (± 0.016)	0.684	0.684	0.674	0.680	0.680
California (20%)(± 0.001)	0.955	0.954	0.954	0.953	0.954
California (10%)(± 0.001)	0.947	0.947	0.947	0.946	0.947
House_16H (± 0.001)	0.948	0.947	0.947	0.947	0.948
House_16H (20%)(± 0.001)	0.946	0.944	0.945	0.944	0.945
House_16H (10%)(± 0.001)	0.939	0.938	0.939	0.937	0.939
House_16H (1%)(± 0.005)	0.899	0.898	0.896	0.898	0.896
Vehicle (± 0.001)	0.994	0.994	0.994	0.994	0.994
Vehicle (10%)(± 0.002)	0.992	0.992	0.992	0.992	0.992
Ionosphere (± 0.003)	0.979	0.977	0.978	0.978	0.979
Ionosphere (20%)(± 0.003)	0.981	0.981	0.984	0.982	0.982
Ionosphere (10%)(± 0.005)	0.965	0.964	0.965	0.966	0.965
Breast Cancer (± 0.001)	0.993	0.993	0.993	0.993	0.993
Breast Cancer (20%)(± 0.001)	0.995	0.995	0.996	0.995	0.996
Breast Cancer (10%)(± 0.001)	0.996	0.996	0.996	0.996	0.996

Table 13: Random Forest (max_depth=tuned with PR AUC) PR AUC for different rebalancing strategies and different data sets.

Strategy	None	CW	RUS	ROS	Near Miss1	BS1	BS2	SMOTE	CV SMOTE	MGS ($d + 1$)
Abalone (1%)	0.048	0.055	0.047	0.049	0.022	0.045	0.041	0.039	0.055	0.035
Phoneme (1%)	0.198	0.215	0.081	0.146	0.054	0.226	0.236	0.236	0.260	0.101
Haberman (10%)	0.246	0.264	0.275	0.227	0.274	0.274	0.287	0.278	0.292	0.283
MagicTel (20%)	0.755	0.759	0.742	0.760	0.336	0.740	0.701	0.756	0.756	0.748

Table 14: Random Forest (max_depth=tuned with PR AUC) PR AUC for different rebalancing strategies and different data sets.

Strategy	None	CW	RUS	ROS	Near Miss 1	BS1	BS2	SMOTE	CV SMOTE	MGS ($d + 1$)
CreditCard (0.2%)	0.849	0.845	0.739	0.846	0.614	0.817	0.808	0.845	0.842	0.837
std	0.003	0.003	0.005	0.003	0.051	0.006	0.009	0.003	0.000	0.002
Phoneme	0.919	0.917	0.885	0.919	0.846	0.911	0.911	0.916	0.914	0.917
std	0.003	0.002	0.005	0.003	0.005	0.004	0.003	0.004	0.004	0.003
Phoneme (20%)	0.863	0.857	0.776	0.861	0.573	0.842	0.844	0.855	0.854	0.855
std	0.004	0.005	0.007	0.005	0.022	0.006	0.005	0.004	0.005	0.005
Phoneme (10%)	0.724	0.707	0.533	0.710	0.268	0.675	0.677	0.695	0.693	0.691
std	0.011	0.012	0.016	0.012	0.018	0.015	0.011	0.010	0.014	0.012
Yeast	0.837	0.843	0.825	0.831	0.712	0.786	0.765	0.831	0.833	0.835
std	0.011	0.006	0.014	0.013	0.019	0.014	0.015	0.008	0.013	0.013
Yeast (1%)	0.351	0.304	0.208	0.269	0.126	0.354	0.301	0.351	0.373	0.316
std	0.055	0.045	0.067	0.055	0.047	0.054	0.051	0.055	0.053	0.060
Wine (4%)	0.602	0.598	0.400	0.588	0.140	0.580	0.572	0.589	0.588	0.536
std	0.023	0.027	0.018	0.028	0.017	0.024	0.024	0.025	0.025	0.027
Pima	0.718	0.709	0.703	0.696	0.701	0.673	0.672	0.689	0.687	0.710
std	0.011	0.008	0.011	0.011	0.009	0.016	0.011	0.015	0.013	0.009
Pima (20%)	0.525	0.522	0.514	0.498	0.490	0.476	0.465	0.484	0.482	0.516
std	0.016	0.020	0.024	0.019	0.013	0.019	0.017	0.017	0.015	0.015
Haberman	0.465	0.479	0.457	0.411	0.468	0.417	0.421	0.431	0.436	0.483
std	0.029	0.024	0.031	0.022	0.017	0.019	0.025	0.024	0.024	0.026
California (20%)	0.888	0.885	0.871	0.886	0.672	0.874	0.862	0.882	0.880	0.879
std	0.001	0.001	0.001	0.002	0.004	0.002	0.002	0.002	0.002	0.002
California (10%)	0.802	0.795	0.760	0.797	0.384	0.774	0.738	0.787	0.784	0.767
std	0.003	0.003	0.004	0.003	0.010	0.004	0.006	0.003	0.003	0.003
California (1%)	0.297	0.290	0.208	0.210	0.019	0.227	0.210	0.249	0.267	0.196
std	0.018	0.018	0.020	0.020	0.002	0.014	0.018	0.021	0.015	0.012
House_16H	0.901	0.896	0.890	0.897	0.799	0.885	0.881	0.892	0.891	0.902
std	0.001	0.001	0.001	0.001	0.002	0.001	0.001	0.001	.001	0.001
House_16H (20%)	0.856	0.847	0.832	0.847	0.578	0.827	0.814	0.837	0.836	0.857
std	0.001	0.001	0.002	0.002	0.005	0.002	0.003	0.001	0.001	0.001
House_16H (10%)	0.757	0.729	0.691	0.731	0.242	0.703	0.680	0.711	0.709	0.756
std	0.003	0.002	0.006	0.003	0.008	0.003	0.006	0.003	0.003	0.002
House_16H (1%)	0.312	0.242	0.167	0.185	0.032	0.208	0.201	0.203	0.212	0.265
std	0.013	0.014	0.018	0.013	0.005	0.011	0.010	0.010	0.011	0.013
Vehicle	0.981	0.978	0.963	0.981	0.957	0.979	0.979	0.978	0.978	0.982
std	0.003	0.003	0.008	0.002	0.006	0.003	0.003	0.003	0.002	0.003
Vehicle (10%)	0.949	0.942	0.869	0.921	0.699	0.932	.935	0.947	0.942	0.944
std	0.010	0.009	0.028	0.014	0.034	0.010	0.012	0.009	0.008	0.009
Ionosphere	0.971	0.970	0.965	0.971	0.932	0.968	0.970	0.968	0.967	0.969
std	0.003	0.003	0.003	0.003	0.007	0.004	0.005	0.005	0.005	0.004
Ionosphere (20%)	0.964	0.955	0.927	0.958	0.730	0.921	0.877	0.925	0.919	0.963
std	0.005	0.007	0.015	0.006	0.022	0.012	0.014	0.010	0.013	0.006
Ionosphere (10%)	0.945	0.917	0.808	0.920	0.526	0.845	0.761	0.820	0.838	0.941
std	0.017	0.019	0.065	0.020	0.065	0.028	0.031	0.033	0.031	0.017
Breast Cancer	0.988	0.986	0.984	0.986	0.987	0.983	0.981	0.986	0.986	0.989
std	0.003	0.003	0.004	0.003	0.003	0.003	0.004	0.004	0.003	0.002
Breast Cancer (20%)	0.984	0.980	0.968	0.979	0.984	0.971	0.967	0.978	0.980	0.985
std	0.005	0.005	0.011	0.008	0.005	0.007	0.009	0.007	0.006	0.005
Breast Cancer (10%)	0.975	0.962	0.939	0.960	0.976	0.936	0.921	0.957	0.954	0.978
std	0.008	0.009	0.014	0.009	0.009	0.016	0.014	0.015	0.015	0.006

1188
1189
1190
1191
1192
1193
1194
1195
1196
1197
1198
1199
1200
1201
1202
1203
1204
1205
1206
1207
1208
1209
1210
1211
1212
1213
1214
1215
1216
1217
1218
1219
1220
1221
1222
1223
1224
1225
1226
1227
1228
1229
1230
1231
1232
1233
1234
1235
1236
1237
1238
1239
1240
1241

Table 15: Highly imbalanced data sets at the top and remaining ones at the bottom. Logistic Regression ROC AUC. For each data set, the best strategy is highlighted in bold and the mean of the standard deviation is computed (and rounded to 10^{-3}).

Strategy	None	CW	RUS	ROS	Near Miss1	BS1	BS2	SMOTE	CV SMOTE	MGS ($d + 1$)
CreditCard (± 0.001)	0.951	0.953	0.963	0.951	0.888	0.903	0.919	0.946	0.955	0.926
Abalone (1%) (± 0.009)	0.848	0.876	0.814	0.878	0.761	0.859	0.853	0.878	0.879	0.872
Phoneme (1%) (± 0.013)	0.800	0.804	0.792	0.804	0.695	0.783	0.779	0.805	0.806	0.805
Yeast (1%) (± 0.006)	0.975	0.974	0.965	0.972	0.920	0.974	0.973	0.973	0.974	0.970
Wine (4%) (± 0.003)	0.836	0.840	0.835	0.839	0.576	0.837	0.831	0.838	0.839	0.833
Pima (20%) (± 0.005)	0.821	0.820	0.813	0.819	0.797	0.818	0.820	0.819	0.819	0.818
Haberman (10%) (± 0.028)	0.751	0.760	0.726	0.758	0.750	0.750	0.746	0.753	0.754	0.743
MagicTel (20%) (± 0.001)	0.844	0.841	0.841	0.841	0.490	0.815	0.814	0.841	0.842	0.838
California (1%) (± 0.004)	0.909	0.922	0.892	0.923	0.648	0.918	0.914	0.925	0.924	0.923
Phoneme (± 0.001)	0.813	0.811	0.811	0.811	0.576	0.801	0.805	0.810	0.812	0.808
Phoneme (20%) (± 0.001)	0.810	0.808	0.807	0.808	0.505	0.801	0.805	0.807	0.809	0.805
Phoneme (10%) (± 0.002)	0.802	0.800	0.799	0.800	0.426	0.796	0.799	0.799	0.801	0.794
Pima (± 0.003)	0.831	0.831	0.828	0.831	0.822	0.829	0.830	0.830	0.830	0.830
Yeast (± 0.001)	0.968	0.967	0.966	0.967	0.945	0.966	0.965	0.967	0.967	0.965
Haberman (± 0.019)	0.674	0.678	0.672	0.674	0.702	0.663	0.661	0.674	0.670	0.674
California (20%) (± 0.001)	0.927	0.927	0.926	0.928	0.903	0.928	0.925	0.928	0.928	0.928
California (10%) (± 0.001)	0.923	0.925	0.921	0.925	0.855	0.925	0.919	0.926	0.926	0.925
House_16H (± 0.001)	0.886	0.889	0.889	0.889	0.867	0.888	0.888	0.889	0.889	0.889
House_16H (20%) (± 0.001)	0.881	0.887	0.887	0.887	0.826	0.886	0.886	0.887	0.887	0.886
House_16H (10%) (± 0.001)	0.871	0.885	0.884	0.885	0.764	0.885	0.885	0.885	0.885	0.883
House_16H (1%) (± 0.006)	0.822	0.862	0.856	0.862	0.694	0.849	0.854	0.861	0.860	0.848
Vehicle (± 0.001)	0.994	0.993	0.990	0.994	0.990	0.993	0.992	0.994	0.994	0.994
Vehicle (10%) (± 0.001)	0.994	0.993	0.985	0.994	0.984	0.993	0.991	0.994	0.994	0.994
Ionosphere (± 0.012)	0.901	0.899	0.904	0.893	0.872	0.889	0.889	0.894	0.895	0.897
Ionosphere (20%) (± 0.021)	0.894	0.886	0.896	0.879	0.872	0.882	0.888	0.881	0.879	0.885
Ionosphere (10%) (± 0.018)	0.862	0.856	0.857	0.858	0.812	0.868	0.878	0.860	0.858	0.862
Breast Cancer (± 0.001)	0.996	0.996	0.996	0.996	0.996	0.996	0.996	0.996	0.996	0.996
Breast Cancer (20%) (± 0.001)	0.997	0.997	0.997	0.997	0.997	0.996	0.994	0.997	0.997	0.997
Breast Cancer (10%) (± 0.001)	0.997	0.997	0.997	0.997	0.996	0.997	0.997	0.997	0.997	0.997

1242

1243

1244

1245

1246

1247

Table 16: Highly imbalanced data sets at the top and remaining ones at the bottom. Logistic regression ROC AUC. For each data set, the best strategy is highlighted in bold and the mean of the standard deviation is computed (and rounded to 10^{-3}).

1248

1249

1250

1251

1252

1253

1254

1255

1256

1257

1258

1259

1260

1261

1262

1263

1264

1265

1266

1267

1268

1269

1270

1271

1272

1273

1274

1275

1276

1277

1278

1279

1280

1281

1282

1283

Table 17: Highly imbalanced data sets ROC AUC. Logistic regression reimplemented in PyTorch using the implementation of Cao et al. (2019).

1284

1285

1286

1287

1288

1289

1290

1291

1292

1293

1294

1295

Strategy	None	LDAM loss	Focal loss
CreditCard	0.968 \pm 0.002	0.934 \pm 0.003	0.967 \pm 0.002
Abalone	0.790 \pm 0.008	0.735 \pm 0.046	0.799 \pm 0.009
Phoneme (1%)	0.806 \pm 0.008	0.656 \pm 0.091	0.807 \pm 0.008
Yeast (1%)	0.977 \pm 0.002	0.942 \pm 0.002	0.977 \pm 0.002
Wine	0.827 \pm 0.002	0.675 \pm 0.087	0.831 \pm 0.002
Pima (20%)	0.821 \pm 0.005	0.697 \pm 0.036	0.821 \pm 0.005
Haberman (10%)	0.749 \pm 0.030	0.611 \pm 0.077	0.750 \pm 0.029
MagicTel (20%)	0.843 \pm 0.001	0.785 \pm 0.20	0.844 \pm 0.001
California (1%)	0.833 \pm 0.006	0.922 \pm 0.003	0.841 \pm 0.007

1296
1297
1298
1299
1300
1301
1302
1303
1304
1305
1306
1307
1308
1309
1310
1311
1312
1313
1314
1315
1316
1317
1318
1319
1320
1321
1322
1323
1324
1325
1326
1327
1328
1329
1330
1331
1332
1333
1334
1335
1336
1337
1338
1339
1340
1341
1342
1343
1344
1345
1346
1347
1348
1349

Table 18: LightGBM PR AUC for different rebalancing strategies and different data sets.

Strategy	None	CW	RUS	ROS	Near Miss1	BS1	BS2	SMOTE	CV SMOTE	MGS ($d + 1$)
CreditCard (0.2%)	0.276	0.772	0.729	0.757	0.334	0.627	0.620	0.724	0.720	0.731
Phoneme (1%)	0.228	0.230	0.054	0.223	0.040	0.263	0.255	0.267	0.278	0.157
House_16H (1%)	0.343	0.362	0.180	0.356	0.023	0.330	0.344	0.312	0.321	0.367

Table 19: LightGBM PR AUC for different rebalancing strategies and different data sets.

Strategy	None	CW	RUS	ROS	Near Miss1	BS1	BS2	SMOTE	CV SMOTE	MGS ($d + 1$)
Abalone (1%)	0.056	0.054	0.047	0.053	0.034	0.050	0.049	0.044	0.045	0.040
std	0.016	0.012	0.015	0.012	0.008	0.011	0.010	0.008	0.008	0.006
Phoneme	0.898	0.895	0.864	0.895	0.733	0.883	0.884	0.894	0.893	0.889
std	0.003	0.003	0.004	0.003	0.014	0.003	0.005	0.003	0.003	0.003
Phoneme (20%)	0.836	0.830	0.757	0.829	0.492	0.814	0.812	0.830	0.828	0.816
std	0.003	0.004	0.008	0.006	0.024	0.007	0.006	0.004	0.006	0.005
Phoneme (10%)	0.683	0.679	0.519	0.680	0.237	0.653	0.657	0.670	0.671	0.643
std	0.012	0.011	0.018	0.013	0.017	0.012	0.011	0.013	0.011	0.014
Yeast	0.795	0.797	0.785	0.801	0.697	0.768	0.761	0.792	0.791	0.793
std	0.017	0.017	0.023	0.016	0.020	0.019	0.020	0.018	0.017	0.017
Yeast (1%)	0.296	0.299	0.010	0.296	0.010	0.330	0.293	0.337	0.334	0.322
std	0.076	0.080	0.000	0.078	0.000	0.072	0.058	0.074	0.068	0.064
Wine (4%)	0.603	0.596	0.269	0.595	0.081	0.545	0.567	0.546	0.534	0.560
std	0.026	0.024	0.019	0.026	0.010	0.022	0.025	0.027	0.022	0.028
Pima	0.666	0.666	0.665	0.672	0.673	0.651	0.658	0.667	0.667	0.672
std	0.014	0.015	0.015	0.012	0.010	0.014	0.017	0.014	0.017	0.012
Pima (20%)	0.475	0.480	0.473	0.473	0.483	0.466	0.470	0.471	0.471	0.466
std	0.019	0.017	0.026	0.016	0.018	0.019	0.021	0.022	0.017	0.019
Haberman	0.433	0.434	0.481	0.410	0.493	0.422	0.423	0.425	0.429	0.418
std	0.026	0.023	0.027	0.022	0.017	0.021	0.021	0.019	0.024	0.027
Haberman (10%)	0.267	0.262	0.140	0.209	0.133	0.255	0.233	0.259	0.272	0.274
std	0.029	0.035	0.028	0.031	0.029	0.035	0.029	0.033	0.030	0.039
MagicTel (20%)	0.761	0.765	0.735	0.765	0.259	0.728	0.729	0.760	0.760	0.750
std	0.003	0.004	0.005	0.004	0.008	0.006	0.005	0.004	0.004	0.004
California (20%)	0.906	0.905	0.891	0.904	0.562	0.895	0.896	0.901	0.902	0.898
std	0.001	0.002	0.002	0.001	0.013	0.002	0.002	0.001	0.001	0.001
California (10%)	0.830	0.831	0.786	0.830	0.314	0.816	0.818	0.823	0.823	0.810
std	0.003	0.003	0.006	0.002	0.012	0.003	0.003	0.003	0.003	0.004
California (1%)	0.359	0.368	0.234	0.343	0.041	0.342	0.322	0.347	0.372	0.285
std	0.019	0.019	0.028	0.023	0.010	0.017	0.018	0.017	0.019	0.020
House_16H	0.911	0.909	0.906	0.909	0.674	0.902	0.901	0.907	0.907	0.910
std	0.001	0.001	0.001	0.001	0.004	0.001	0.001	0.001	0.001	0.001
House_16H (20%)	0.869	0.867	0.857	0.866	0.417	0.855	0.854	0.862	0.861	0.868
std	0.002	0.001	0.002	0.001	0.005	0.001	0.002	0.001	0.001	0.001
House_16H (10%)	0.776	0.770	0.735	0.769	0.174	0.751	0.752	0.757	0.755	0.775
std	0.002	0.003	0.006	0.002	0.004	0.003	0.003	0.003	0.003	0.002
Vehicle	0.989	0.989	0.974	0.988	0.903	0.989	0.990	0.988	0.988	0.980
std	0.003	0.003	0.008	0.003	0.011	0.003	0.003	0.003	0.002	0.004
Vehicle (10%)	0.958	0.954	0.857	0.948	0.392	0.954	0.942	0.954	0.955	0.954
std	0.012	0.011	0.033	0.013	0.060	0.012	0.012	0.011	0.011	0.010
Ionosphere	0.968	0.967	0.958	0.965	0.937	0.962	0.967	0.963	0.963	0.967
std	0.004	0.005	0.004	0.005	0.009	0.006	0.005	0.006	0.006	0.004
Ionosphere (20%)	0.953	0.953	0.898	0.952	0.798	0.937	0.943	0.930	0.933	0.953
std	0.013	0.011	0.016	0.012	0.022	0.012	0.010	0.011	0.013	0.008
Ionosphere (10%)	0.895	0.895	0.456	0.882	0.431	0.865	0.868	0.827	0.840	0.903
std	0.027	0.024	0.080	0.024	0.085	0.027	0.027	0.026	0.028	0.019
Breast cancer	0.989	0.990	0.986	0.989	0.987	0.988	0.987	0.990	0.989	0.991
std	0.003	0.002	0.004	0.002	0.004	0.002	0.003	0.002	0.003	0.002
Breast cancer (20%)	0.980	0.981	0.974	0.980	0.981	0.976	0.972	0.979	0.977	0.984
std	0.005	0.005	0.008	0.007	0.005	0.008	0.008	0.006	0.007	0.005
Breast cancer (10%)	0.972	0.973	0.926	0.973	0.967	0.965	0.962	0.973	0.970	0.975
std	0.011	0.010	0.019	0.010	0.008	0.014	0.015	0.011	0.013	0.010

1404
1405
1406
1407
1408
1409
1410
1411
1412
1413
1414
1415
1416
1417
1418
1419
1420
1421
1422
1423
1424
1425
1426
1427
1428
1429
1430
1431
1432
1433
1434
1435
1436
1437
1438
1439
1440
1441
1442
1443
1444
1445
1446
1447
1448
1449
1450
1451
1452
1453
1454
1455
1456
1457

Table 20: LightGBM ROC AUC for different rebalancing strategies and different data sets.

Strategy	None	CW	RUS	ROS	Near Miss1	BS1	BS2	SMOTE	CV SMOTE	MGS ($d + 1$)
CreditCard (0.2%)	0.761	0.938	0.970	0.921	0.879	0.941	0.932	0.937	0.950	0.956
std	0.000	0.000	0.000	0.000	0.000	0.000	0.000	0.017	0.000	0.002
Abalone (1%)	0.738	0.738	0.726	0.738	0.700	0.750	0.757	0.748	0.775	0.745
std	0.029	0.029	0.018	0.023	0.030	0.019	0.021	0.020	0.015	0.016
Phoneme	0.954	0.953	0.943	0.953	0.863	0.949	0.950	0.952	0.952	0.951
std	0.001	0.001	0.001	0.001	0.006	0.001	0.002	0.001	0.001	0.001
Phoneme (20%)	0.946	0.945	0.929	0.944	0.761	0.942	0.942	0.945	0.942	0.942
std	0.001	0.001	0.002	0.002	0.014	0.002	0.002	0.001	0.002	0.001
Phoneme (10%)	0.930	0.928	0.907	0.929	0.628	0.923	0.926	0.925	0.926	0.925
std	0.003	0.003	0.005	0.004	0.014	0.003	0.003	0.004	0.003	0.003
Phoneme (1%)	0.898	0.878	0.828	0.836	0.706	0.889	0.883	0.895	0.885	0.888
std	0.014	0.022	0.021	0.028	0.042	0.013	0.022	0.014	0.017	0.018
Yeast	0.966	0.966	0.966	0.968	0.923	0.968	0.968	0.968	0.968	0.967
std	0.003	0.003	0.004	0.003	0.006	0.002	0.003	0.002	0.002	0.003
Yeast (1%)	0.930	0.933	0.500	0.847	0.500	0.927	0.928	0.927	0.923	0.915
std	0.025	0.023	0.000	0.069	0.000	0.025	0.027	0.025	0.022	0.028
Wine (4%)	0.927	0.922	0.906	0.918	0.682	0.920	0.924	0.920	0.920	0.923
std	0.006	0.008	0.007	0.010	0.013	0.008	0.007	0.008	0.006	0.008
Pima	0.803	0.802	0.798	0.806	0.789	0.800	0.801	0.804	0.805	0.807
std	0.008	0.007	0.008	0.007	0.006	0.008	0.008	0.009	0.009	0.008
Pima (20%)	0.773	0.772	0.772	0.772	0.762	0.782	0.784	0.780	0.780	0.771
std	0.011	0.010	0.014	0.009	0.009	0.012	0.010	0.012	0.010	0.010
Haberman	0.684	0.687	0.707	0.668	0.707	0.680	0.677	0.685	0.681	0.666
std	0.018	0.018	0.018	0.018	0.013	0.019	0.019	0.017	0.017	0.019
Haberman (10%)	0.691	0.689	0.575	0.643	0.564	0.710	0.674	0.712	0.726	0.729
std	0.031	0.034	0.063	0.030	0.052	0.030	0.040	0.026	0.030	0.025
MagicTel (20%)	0.923	0.925	0.917	0.924	0.622	0.918	0.918	0.922	0.922	0.917
std	0.001	0.001	0.001	0.001	0.004	0.001	0.001	0.001	0.001	0.001
California (20%)	0.964	0.963	0.960	0.963	0.833	0.960	0.961	0.962	0.962	0.960
std	0.001	0.001	0.001	0.001	0.004	0.001	0.001	0.001	0.001	0.001
California (10%)	0.957	0.957	0.949	0.956	0.771	0.954	0.954	0.955	0.955	0.949
std	0.001	0.001	0.002	0.001	0.005	0.001	0.001	0.001	0.001	0.002
California (1%)	0.911	0.908	0.890	0.906	0.663	0.910	0.907	0.907	0.912	0.884
std	0.007	0.006	0.010	0.007	0.017	0.009	0.009	0.007	0.005	0.012
House_16H	0.954	0.954	0.953	0.953	0.874	0.950	0.950	0.953	0.953	0.954
std	0.000	0.000	0.001	0.000	0.001	0.000	0.000	0.000	0.000	0.000
House_16H (20%)	0.953	0.953	0.951	0.953	0.794	0.949	0.949	0.951	0.951	0.953
std	0.000	0.000	0.001	0.000	0.002	0.000	0.000	0.000	0.000	0.000
House_16H (10%)	0.950	0.949	0.945	0.949	0.686	0.945	0.946	0.945	0.944	0.950
std	0.001	0.001	0.001	0.001	0.003	0.001	0.001	0.001	0.001	0.001
House_16H (1%)	0.903	0.896	0.899	0.896	0.605	0.907	0.909	0.894	0.894	0.912
std	0.005	0.007	0.005	0.006	0.013	0.005	0.006	0.005	0.004	0.005
Vehicle	0.996	0.996	0.992	0.996	0.949	0.996	0.997	0.996	0.996	0.996
std	0.001	0.001	0.002	0.001	0.006	0.001	0.001	0.001	0.001	0.001
Vehicle (10%)	0.993	0.992	0.978	0.990	0.794	0.993	0.991	0.992	0.992	0.992
std	0.003	0.004	0.005	0.008	0.020	0.003	0.003	0.006	0.005	0.002
Ionosphere	0.973	0.973	0.967	0.972	0.944	0.971	0.975	0.972	0.972	0.974
std	0.004	0.005	0.005	0.004	0.006	0.005	0.004	0.005	0.004	0.005
Ionosphere (20%)	0.981	0.980	0.962	0.980	0.887	0.978	0.980	0.974	0.975	0.981
std	0.006	0.005	0.007	0.007	0.012	0.006	0.006	0.005	0.007	0.004
Ionosphere (10%)	0.972	0.972	0.777	0.959	0.753	0.954	0.951	0.927	0.946	0.975
std	0.010	0.013	0.048	0.017	0.057	0.013	0.013	0.015	0.013	0.007
Breast cancer	0.995	0.995	0.994	0.995	0.994	0.994	0.994	0.995	0.995	0.995
std	0.001	0.001	0.001	0.001	0.001	0.001	0.001	0.001	0.001	0.001
Breast cancer (20%)	0.996	0.996	0.994	0.996	0.996	0.995	0.995	0.996	0.996	0.997
std	0.001	0.001	0.001	0.001	0.001	0.001	0.001	0.001	0.001	0.001

B MAIN PROOFS

This section contains the main proof of our theoretical results. The technical lemmas used by several proofs are available on Appendix C.

B.1 PROOF OF LEMMA 3.1

Proof of Lemma 3.1. Let \mathcal{X} be the support of P_X . SMOTE generates new points by linear interpolation of the original minority sample. This means that for all x, y in the minority samples or generated by SMOTE procedure, we have $(1-t)x + ty \in \text{Conv}(\mathcal{X})$ by definition of $\text{Conv}(\mathcal{X})$. This leads to the fact that precisely, all the new SMOTE samples are contained in $\text{Conv}(\mathcal{X})$. This implies $\text{Supp}(P_Z) \subseteq \text{Conv}(\mathcal{X})$. □

B.2 PROOF OF THEOREM 3.2

Proof of Theorem 3.2. For any event A, B , we have

$$1 - \mathbb{P}[A \cap B] = \mathbb{P}[A^c \cup B^c] \leq \mathbb{P}[A^c] + \mathbb{P}[B^c], \quad (8)$$

which leads to

$$\mathbb{P}[A \cap B] \geq 1 - \mathbb{P}[A^c] - \mathbb{P}[B^c] \quad (9)$$

$$= \mathbb{P}[A] - \mathbb{P}[B^c]. \quad (10)$$

By construction,

$$\|X_c - Z\| \leq \|X_c - X_{(K)}(X_c)\|. \quad (11)$$

Let $x \in \mathcal{X}$ and $\eta > 0$. Let $\alpha, \varepsilon > 0$. We have,

$$\mathbb{P}[X_c \in B(x, \alpha - \varepsilon)] - \mathbb{P}[\|X_c - X_{(K)}(X_c)\| > \varepsilon] \quad (12)$$

$$\leq \mathbb{P}[X_c \in B(x, \alpha - \varepsilon), \|X_c - X_{(K)}(X_c)\| \leq \varepsilon] \quad (13)$$

$$\leq \mathbb{P}[X_c \in B(x, \alpha - \varepsilon), \|X_c - Z\| \leq \varepsilon] \quad (14)$$

$$\leq \mathbb{P}[Z \in B(x, \alpha)]. \quad (15)$$

Similarly, we have

$$\mathbb{P}[Z \in B(x, \alpha)] - \mathbb{P}[\|X_c - X_{(K)}(X_c)\| > \varepsilon] \quad (16)$$

$$\leq \mathbb{P}[Z \in B(x, \alpha), \|X_c - X_{(K)}(X_c)\| \leq \varepsilon] \quad (17)$$

$$\leq \mathbb{P}[Z \in B(x, \alpha), \|X_c - Z\| \leq \varepsilon] \quad (18)$$

$$\leq \mathbb{P}[X_c \in B(x, \alpha + \varepsilon)]. \quad (19)$$

Since X_c admits a density, for all $\varepsilon > 0$ small enough

$$\mathbb{P}[X_c \in B(x, \alpha + \varepsilon)] \leq \mathbb{P}[X_c \in B(x, \alpha)] + \eta, \quad (20)$$

and

$$\mathbb{P}[X_c \in B(x, \alpha)] - \eta \leq \mathbb{P}[X_c \in B(x, \alpha - \varepsilon)]. \quad (21)$$

Let ε such that equation 20 and equation 21 are verified. According to Lemma 2.3 in Biau & Devroye (2015), since X_1, \dots, X_n are i.i.d., if K/n tends to zero as $n \rightarrow \infty$, we have

$$\mathbb{P}[\|X_c - X_{(K)}(X_c)\| > \varepsilon] \rightarrow 0. \quad (22)$$

Thus, for all n large enough,

$$\mathbb{P}[X_c \in B(x, \alpha)] - 2\eta \leq \mathbb{P}[Z \in B(x, \alpha)] \quad (23)$$

and

$$\mathbb{P}[Z \in B(x, \alpha)] \leq 2\eta + \mathbb{P}[X_c \in B(x, \alpha)]. \quad (24)$$

Finally, for all $\eta > 0$, for all n large enough, we obtain

$$\mathbb{P}[X_c \in B(x, \alpha)] - 2\eta \leq \mathbb{P}[Z \in B(x, \alpha)] \leq 2\eta + \mathbb{P}[X_c \in B(x, \alpha)], \quad (25)$$

which proves that

$$\mathbb{P}[Z \in B(x, \alpha)] \rightarrow \mathbb{P}[X_c \in B(x, \alpha)]. \quad (26)$$

Therefore, by the Monotone convergence theorem, for all Borel sets $B \subset \mathbb{R}^d$,

$$\mathbb{P}[Z \in B] \rightarrow \mathbb{P}[X_c \in B]. \quad (27)$$

□

1512 B.3 PROOF OF LEMMA 3.3
1513

1514 *Proof of Lemma 3.3.* We consider a single SMOTE iteration. Recall that the central point X_c (see
1515 Algorithm 1) is fixed, and thus denoted by x_c .

1516 The random variables $X_{(1)}(x_c), \dots, X_{(n-1)}(x_c)$ denote a reordering of the initial observations $X -$
1517 $1, X_2, \dots, X_n$ such that

$$1518 \quad \|X_{(1)}(x_c) - x_c\| \leq \|X_{(2)}(x_c) - x_c\| \leq \dots \leq \|X_{(n-1)}(x_c) - x_c\|.$$

1520 For clarity, we remove the explicit dependence on x_c . Recall that SMOTE builds a linear interpo-
1521 lation between x_c and one of its K nearest neighbors chosen uniformly. Then the newly generated
1522 point Z satisfies

$$1523 \quad Z = (1 - W)x_c + W \sum_{k=1}^K X_{(k)} \mathbb{1}_{\{I=k\}}, \quad (28)$$

1524 where W is a uniform random variable over $[0, 1]$, independent of I, X_1, \dots, X_n , with I distributed
1525 as $\mathcal{U}(\{1, \dots, K\})$.

1528 From now, consider that the k -th nearest neighbor of x_c , $X_{(k)}(x_c)$, has been chosen (that is $I = k$).
1529 Then Z satisfies

$$1530 \quad Z = (1 - W)x_c + WX_{(k)} \quad (29)$$

$$1531 \quad = x_c - Wx_c + WX_{(k)}, \quad (30)$$

1533 which implies

$$1534 \quad Z - x_c = W(X_{(k)} - x_c). \quad (31)$$

1536 Let f_{Z-x_c}, f_W and $f_{X_{(k)}-x_c}$ be respectively the density functions of $Z - x_c, W$ and $X_{(k)} - x_c$. Let
1537 $z, z_1, z_2 \in \mathbb{R}^d$. Recall that $z \leq z_1$ means that each component of z is lower than the corresponding
1538 component of z_1 . Since W and $X_{(k)} - x_c$ are independent, we have,

$$1540 \quad \mathbb{P}(z_1 \leq Z - x_c \leq z_2) = \int_{w \in \mathbb{R}} \int_{x \in \mathbb{R}^d} f_{W, X_{(k)}-x_c}(w, x) \mathbb{1}_{\{z_1 \leq wx \leq z_2\}} dw dx \quad (32)$$

$$1541 \quad = \int_{w \in \mathbb{R}} \int_{x \in \mathbb{R}^d} f_W(w) f_{X_{(k)}-x_c}(x) \mathbb{1}_{\{z_1 \leq wx \leq z_2\}} dw dx \quad (33)$$

$$1542 \quad = \int_{w \in \mathbb{R}} f_W(w) \left(\int_{x \in \mathbb{R}^d} f_{X_{(k)}-x_c}(x) \mathbb{1}_{\{z_1 \leq wx \leq z_2\}} dx \right) dw. \quad (34)$$

1543 Besides, let $u = wx$. Then $x = (\frac{u_1}{w}, \dots, \frac{u_d}{w})^T$. The Jacobian of such transformation equals:

$$1544 \quad \begin{vmatrix} \frac{\partial x_1}{\partial u_1} & \dots & \frac{\partial x_1}{\partial u_d} \\ \vdots & \ddots & \vdots \\ \frac{\partial x_d}{\partial u_1} & \dots & \frac{\partial x_d}{\partial u_d} \end{vmatrix} = \begin{vmatrix} \frac{1}{w} & & 0 \\ & \ddots & \\ 0 & \dots & \frac{1}{w} \end{vmatrix} = \frac{1}{w^d} \quad (35)$$

1545 Therefore, we have $x = u/w$ and $dx = du/w^d$, which leads to

$$1546 \quad \mathbb{P}(z_1 \leq Z - x_c \leq z_2) \quad (36)$$

$$1547 \quad = \int_{w \in \mathbb{R}} \frac{1}{w^d} f_W(w) \left(\int_{u \in \mathbb{R}^d} f_{X_{(k)}-x_c} \left(\frac{u}{w} \right) \mathbb{1}_{\{z_1 \leq u \leq z_2\}} du \right) dw. \quad (37)$$

1548 Note that a random variable Z' with density function

$$1549 \quad f_{Z'}(z') = \int_{w \in \mathbb{R}} \frac{1}{w^d} f_W(w) f_{X_{(k)}-x_c} \left(\frac{z'}{w} \right) dw \quad (38)$$

1550 satisfies, for all $z_1, z_2 \in \mathbb{R}^d$,

$$1551 \quad \mathbb{P}(z_1 \leq Z - x_c \leq z_2) = \int_{w \in \mathbb{R}} \frac{1}{w^d} f_W(w) \left(\int_{u \in \mathbb{R}^d} f_{X_{(k)}-x_c} \left(\frac{u}{w} \right) \mathbb{1}_{\{z_1 \leq u \leq z_2\}} du \right) dw. \quad (39)$$

Therefore, the variable $Z - x_c$ admits the following density

$$f_{Z-x_c}(z'|X_c = x_c, I = k) = \int_{w \in \mathbb{R}} \frac{1}{w^d} f_W(w) f_{X_{(k)}-x_c}\left(\frac{z'}{w}\right) dw. \quad (40)$$

Since W follows a uniform distribution on $[0, 1]$, we have

$$f_{Z-x_c}(z'|X_c = x_c, I = k) = \int_0^1 \frac{1}{w^d} f_{X_{(k)}-x_c}\left(\frac{z'}{w}\right) dw. \quad (41)$$

The density $f_{X_{(k)}-x_c}$ of the k -th nearest neighbor of x_c can be computed exactly (see, Lemma 6.1 in Berrett, 2017), that is

$$\begin{aligned} f_{X_{(k)}-x_c}(u) &= (n-1) \binom{n-2}{k-1} f_X(x_c + u) [\mu_X(B(x_c, \|u\|))]^{k-1} \\ &\quad \times [1 - \mu_X(B(x_c, \|u\|))]^{n-k-1}, \end{aligned} \quad (42)$$

where

$$\mu_X(B(x_c, \|u\|)) = \int_{B(x_c, \|u\|)} f_X(x) dx. \quad (43)$$

We recall that $B(x_c, \|u\|)$ is the ball centered on x_c and of radius $\|u\|$. Hence we have

$$f_{X_{(k)}-x_c}(u) = (n-1) \binom{n-2}{k-1} f_X(x_c + u) \mu_X(B(x_c, \|u\|))^{k-1} [1 - \mu_X(B(x_c, \|u\|))]^{n-k-1}. \quad (44)$$

Since $Z - x_c$ is a translation of the random variable Z , we have

$$f_Z(z|X_c = x_c, I = k) = f_{Z-x_c}(z - x_c|X_c = x_c, I = k). \quad (45)$$

Injecting Equation (44) in Equation (41), we obtain

$$f_Z(z|X_c = x_c, I = k) \quad (46)$$

$$= f_{Z-x_c}(z - x_c|X_c = x_c, I = k) \quad (47)$$

$$= \int_0^1 \frac{1}{w^d} f_{X_{(k)}-x_c}\left(\frac{z - x_c}{w}\right) dw \quad (48)$$

$$= (n-1) \binom{n-2}{k-1} \int_0^1 \frac{1}{w^d} f_X\left(x_c + \frac{z - x_c}{w}\right) \mu_X\left(B\left(x_c, \frac{\|z - x_c\|}{w}\right)\right)^{k-1} \quad (49)$$

$$\times \left[1 - \mu_X\left(B\left(x_c, \frac{\|z - x_c\|}{w}\right)\right)\right]^{n-k-1} dw \quad (50)$$

Recall that in SMOTE, k is chosen at random in $\{1, \dots, K\}$ through the uniform random variable I . So far, we have considered I fixed. Taking the expectation with respect to I , we have

$$f_Z(z|X_c = x_c) \quad (51)$$

$$= \sum_{k=1}^K f_Z(z|X_c = x_c, I = k) \mathbb{P}[I = k] \quad (52)$$

$$= \frac{1}{K} \sum_{k=1}^K \int_0^1 \frac{1}{w^d} f_{X^{(k)} - x_c} \left(\frac{z - x_c}{w} \right) dw \quad (53)$$

$$= \frac{1}{K} \sum_{k=1}^K (n-1) \binom{n-2}{k-1} \int_0^1 \frac{1}{w^d} f_X \left(x_c + \frac{z - x_c}{w} \right) \mu_X \left(B \left(x_c, \frac{\|z - x_c\|}{w} \right) \right)^{k-1} \quad (54)$$

$$\times \left[1 - \mu_X \left(B \left(x_c, \frac{\|z - x_c\|}{w} \right) \right) \right]^{n-k-1} dw \quad (55)$$

$$= \frac{(n-1)}{K} \int_0^1 \frac{1}{w^d} f_X \left(x_c + \frac{z - x_c}{w} \right) \sum_{k=1}^K \binom{n-2}{k-1} \mu_X \left(B \left(x_c, \frac{\|z - x_c\|}{w} \right) \right)^{k-1} \quad (56)$$

$$\times \left[1 - \mu_X \left(B \left(x_c, \frac{\|z - x_c\|}{w} \right) \right) \right]^{n-k-1} dw \quad (57)$$

$$= \frac{(n-1)}{K} \int_0^1 \frac{1}{w^d} f_X \left(x_c + \frac{z - x_c}{w} \right) \sum_{k=0}^{K-1} \binom{n-2}{k} \mu_X \left(B \left(x_c, \frac{\|z - x_c\|}{w} \right) \right)^k \quad (58)$$

$$\times \left[1 - \mu_X \left(B \left(x_c, \frac{\|z - x_c\|}{w} \right) \right) \right]^{n-k-2} dw. \quad (59)$$

Note that the sum can be expressed as the cumulative distribution function of a Binomial distribution parameterized by $n-2$ and $\mu_X(B(x_c, \|z-x_c\|/w))$, so that

$$\sum_{k=0}^{K-1} \binom{n-2}{k} \mu_X \left(B \left(x_c, \frac{\|z - x_c\|}{w} \right) \right)^k \left[1 - \mu_X \left(B \left(x_c, \frac{\|z - x_c\|}{w} \right) \right) \right]^{n-k-2} \quad (60)$$

$$= (n-K-1) \binom{n-2}{K-1} \mathcal{B} \left(n-K-1, K; 1 - \mu_X \left(B \left(x_c, \frac{\|z - x_c\|}{w} \right) \right) \right), \quad (61)$$

(see Technical Lemma C.1 for details). We inject Equation (61) in Equation (51)

$$f_Z(z|X_c = x_c) = (n-K-1) \binom{n-1}{K} \int_0^1 \frac{1}{w^d} f_X \left(x_c + \frac{z - x_c}{w} \right) \times \mathcal{B} \left(n-K-1, K; 1 - \mu_X \left(B \left(x_c, \frac{\|z - x_c\|}{w} \right) \right) \right) dw. \quad (62)$$

We know that

$$f_Z(z) = \int_{x_c \in \mathcal{X}} f_Z(z|X_c = x_c) f_X(x_c) dx_c.$$

Combining this remark with the result of Equation (62) we get

$$f_Z(z) = (n-K-1) \binom{n-1}{K} \int_{x_c \in \mathcal{X}} \int_0^1 \frac{1}{w^d} f_X \left(x_c + \frac{z - x_c}{w} \right) \times \mathcal{B} \left(n-K-1, K; 1 - \mu_X \left(B \left(x_c, \frac{\|z - x_c\|}{w} \right) \right) \right) f_X(x_c) dw dx_c. \quad (63)$$

Link with Elreedy's formula According to the Elreedy formula

$$f_Z(z|X_c = x_c) = (n-K-1) \binom{n-1}{K} \int_{r=\|z-x_c\|}^{\infty} f_X \left(x_c + \frac{(z-x_c)r}{\|z-x_c\|} \right) \frac{r^{d-2}}{\|z-x_c\|^{d-1}} \times \mathcal{B}(n-K-1, K; 1 - \mu_X(B(x_c, r))) dr. \quad (64)$$

Now, let $r = \|z - x_c\|/w$ so that $dr = -\|z - x_c\|dw/w^2$. Thus,

$$f_Z(z|X_c = x_c) = (n - K - 1) \binom{n-1}{K} \int_0^1 f_X \left(x_c + \frac{z - x_c}{w} \right) \frac{1}{w^{d-2}} \frac{1}{\|z - x_c\|} \quad (65)$$

$$\times \mathcal{B} \left(n - K - 1, K; 1 - \mu_X \left(B \left(x_c, \frac{z - x_c}{w} \right) \right) \right) \frac{\|z - x_c\|}{w^2} dw \quad (66)$$

$$= (n - K - 1) \binom{n-1}{K} \int_0^1 \frac{1}{w^d} f_X \left(x_c + \frac{z - x_c}{w} \right) \times \mathcal{B} \left(n - K - 1, K; 1 - \mu_X \left(B \left(x_c, \frac{z - x_c}{w} \right) \right) \right) dw. \quad (67)$$

□

B.4 PROOF OF THEOREM 3.5

Proof of Theorem 3.5. Let $x_c \in \mathcal{X}$ be a central point in a SMOTE iteration. From Lemma 3.3, we have,

$$f_Z(z|X_c = x_c) = (n - K - 1) \binom{n-1}{K} \int_0^1 \frac{1}{w^d} f_X \left(x_c + \frac{z - x_c}{w} \right) \times \mathcal{B} \left(n - K - 1, K; 1 - \mu_X \left(B \left(x_c, \frac{\|z - x_c\|}{w} \right) \right) \right) dw \quad (68)$$

$$= (n - K - 1) \binom{n-1}{K} \int_0^1 \frac{1}{w^d} f_X \left(x_c + \frac{z - x_c}{w} \right) \mathbb{1}_{\{x_c + \frac{z - x_c}{w} \in \mathcal{X}\}} \times \mathcal{B} \left(n - K - 1, K; 1 - \mu_X \left(B \left(x_c, \frac{\|z - x_c\|}{w} \right) \right) \right) dw. \quad (69)$$

Let $R \in \mathbb{R}$ such that $\mathcal{X} \subset \mathcal{B}(0, R)$. For all $u = x_c + \frac{z - x_c}{w}$, we have

$$w = \frac{\|z - x_c\|}{\|u - x_c\|}. \quad (70)$$

If $u \in \mathcal{X}$, then $u \in \mathcal{B}(0, R)$. Besides, since $x_c \in \mathcal{X} \subset \mathcal{B}(0, R)$, we have $\|u - x_c\| < 2R$ and

$$w > \frac{\|z - x_c\|}{2R}. \quad (71)$$

Consequently,

$$\mathbb{1}_{\{x_c + \frac{z - x_c}{w} \in \mathcal{X}\}} \leq \mathbb{1}_{\{w > \frac{\|z - x_c\|}{2R}\}}. \quad (72)$$

So finally

$$\mathbb{1}_{\{x_c + \frac{z - x_c}{w} \in \mathcal{X}\}} = \mathbb{1}_{\{x_c + \frac{z - x_c}{w} \in \mathcal{X}\}} \mathbb{1}_{\{w > \frac{\|z - x_c\|}{2R}\}}. \quad (73)$$

Hence,

$$f_Z(z|X_c = x_c) = (n - K - 1) \binom{n-1}{K} \int_0^1 \frac{1}{w^d} f_X \left(x_c + \frac{z - x_c}{w} \right) \mathbb{1}_{\{x_c + \frac{z - x_c}{w} \in \mathcal{X}\}} \mathbb{1}_{\{w > \frac{\|z - x_c\|}{2R}\}} \times \mathcal{B} \left(n - K - 1, K; 1 - \mu_X \left(B \left(x_c, \frac{\|z - x_c\|}{w} \right) \right) \right) dw \quad (74)$$

$$= (n - K - 1) \binom{n-1}{K} \int_{\frac{\|z - x_c\|}{2R}}^1 \frac{1}{w^d} f_X \left(x_c + \frac{z - x_c}{w} \right) \times \mathcal{B} \left(n - K - 1, K; 1 - \mu_X \left(B \left(x_c, \frac{\|z - x_c\|}{w} \right) \right) \right) dw. \quad (75)$$

Now, let $0 < \alpha \leq 2R$ and $z \in \mathbb{R}^d$ such that $\|z - x_c\| > \alpha$. In such a case, $w > \frac{\alpha}{2R}$ and:

$$f_Z(z|X_c = x_c) \quad (76)$$

$$\begin{aligned} &= (n - K - 1) \binom{n-1}{K} \int_{\frac{\alpha}{2R}}^1 \frac{1}{w^d} f_X \left(x_c + \frac{z - x_c}{w} \right) \\ &\quad \times \mathcal{B} \left(n - K - 1, K; 1 - \mu_X \left(B \left(x_c, \frac{\|z - x_c\|}{w} \right) \right) \right) dw \end{aligned} \quad (77)$$

$$\leq (n - K - 1) \binom{n-1}{K} \int_{\frac{\alpha}{2R}}^1 \frac{1}{w^d} f_X \left(x_c + \frac{z - x_c}{w} \right) \mathcal{B}(n - K - 1, K; 1 - \mu_X(B(x_c, \alpha))) dw. \quad (78)$$

Let $\mu \in [0, 1]$ and S_n be a binomial random variable of parameters $(n - 1, \mu)$. For all K ,

$$\mathbb{P}[S_n \leq K] = (n - K - 1) \binom{n-1}{K} \mathcal{B}(n - K - 1, K; 1 - \mu). \quad (79)$$

According to Hoeffding's inequality, we have, for all $K \leq (n - 1)\mu$,

$$\mathbb{P}[S_n \leq K] \leq \exp \left(-2(n - 1) \left(\mu - \frac{K}{n - 1} \right)^2 \right). \quad (80)$$

Thus, for all $z \notin B(x_c, \alpha)$, for all $K \leq (n - 1)\mu_X(B(x_c, \alpha))$,

$$f_Z(z|X_c = x_c) \quad (81)$$

$$\leq \exp \left(-2(n - 1) \left(\mu_X(B(x_c, \alpha)) - \frac{K}{n - 1} \right)^2 \right) \int_{\frac{\alpha}{2R}}^1 \frac{1}{w^d} f_X \left(x_c + \frac{z - x_c}{w} \right) dw \quad (82)$$

$$\leq C_2 \exp \left(-2(n - 1) \left(\mu_X(B(x_c, \alpha)) - \frac{K}{n - 1} \right)^2 \right) \int_{\frac{\alpha}{2R}}^1 \frac{1}{w^d} dw \quad (83)$$

$$\leq C_2 \eta(\alpha, R) \exp \left(-2(n - 1) \left(\mu_X(B(x_c, \alpha)) - \frac{K}{n - 1} \right)^2 \right), \quad (84)$$

with

$$\eta(\alpha, R) = \begin{cases} \ln \left(\frac{2R}{\alpha} \right) & \text{if } d = 1 \\ \frac{1}{d-1} \left(\left(\frac{2R}{\alpha} \right)^{d-1} - 1 \right) & \text{otherwise} \end{cases}.$$

Letting

$$\epsilon(n, \alpha, K, x_c) = C_2 \eta(\alpha, R) \exp \left(-2(n - 1) \left(\mu_X(B(x_c, \alpha)) - \frac{K}{n - 1} \right)^2 \right), \quad (85)$$

we have, for all $\alpha \in (0, 2R)$, for all $K \leq (n - 1)\mu_X(B(x_c, \alpha))$,

$$\mathbb{P}(|Z - X_c| \geq \alpha | X_c = x_c) = \int_{z \notin B(x_c, \alpha), z \in \mathcal{X}} f_Z(z|X_c = x_c) dz \quad (86)$$

$$\leq \int_{z \notin B(x_c, \alpha), z \in \mathcal{X}} \epsilon(n, \alpha, K, x_c) dz \quad (87)$$

$$= \epsilon(n, \alpha, K, x_c) \int_{z \notin B(x_c, \alpha), z \in \mathcal{X}} dz \quad (88)$$

$$\leq c_d R^d \epsilon(n, \alpha, K, x_c), \quad (89)$$

as $\mathcal{X} \subset B(0, R)$. Since $x_c \in \mathcal{X}$, by definition of the support, we know that for all $\rho > 0$, $\mu_X(B(x_c, \rho)) > 0$. Thus, $\mu_X(B(x_c, \alpha)) > 0$. Consequently, $\epsilon(n, \alpha, K, x_c)$ tends to zero, as K/n tends to zero. \square

1782 B.5 PROOF OF COROLLARY 3.6
1783

1784 We adapt the proof of Theorem 2.1 and Theorem 2.4 in Biau & Devroye (2015) to the case where
1785 X belongs to $B(0, R)$. We prove the following result.

1786 **Lemma B.1.** *Let X takes values in $B(0, R)$. For all $d \geq 2$,*
1787

$$1788 \mathbb{E}[\|X_{(1)}(X) - X\|_2^2] \leq 36R^2 \left(\frac{k}{n+1}\right)^{2/d}, \quad (90)$$

1791 where $X_{(1)}(X)$ is the nearest neighbor of X among X_1, \dots, X_n .

1793 *Proof of Lemma B.1.* Let us denote by $X_{(i,1)}$ the nearest neighbor of X_i among
1794 $X_1, \dots, X_{i-1}, X_{i+1}, \dots, X_{n+1}$. By symmetry, we have

$$1796 \mathbb{E}[\|X_{(1)}(X) - X\|_2^2] = \frac{1}{n+1} \sum_{i=1}^{n+1} \mathbb{E}\|X_{(i,1)} - X_i\|_2^2. \quad (91)$$

1799 Let $R_i = \|X_{(i,1)} - X_i\|_2$ and $B_i = \{x \in \mathbb{R}^d : \|x - X_i\| < R_i/2\}$. By construction, B_i are disjoint.
1800 Since $R_i \leq 2R$, we have

$$1801 \cup_{i=1}^{n+1} B_i \subset B(0, 3R), \quad (92)$$

1803 which implies,

$$1804 \mu\left(\cup_{i=1}^{n+1} B_i\right) \leq (3R)^d c_d. \quad (93)$$

1806 Thus, we have

$$1807 \sum_{i=1}^{n+1} c_d \left(\frac{R_i}{2}\right)^d \leq (3R)^d c_d. \quad (94)$$

1811 Besides, for all $d \geq 2$, we have

$$1812 \left(\frac{1}{n+1} \sum_{i=1}^{n+1} R_i^2\right)^{d/2} \leq \frac{1}{n+1} \sum_{i=1}^{n+1} R_i^d, \quad (95)$$

1816 which leads to

$$1817 \mathbb{E}[\|X_{(1)}(X) - X\|_2^2] = \frac{1}{n+1} \sum_{i=1}^{n+1} \mathbb{E}\|X_{(i,1)} - X_i\|_2^2 \quad (96)$$

$$1818 = \mathbb{E}\left[\frac{1}{n+1} \sum_{i=1}^{n+1} R_i^2\right] \quad (97)$$

$$1819 \leq \left(\frac{(6R)^d}{n+1}\right)^{2/d} \quad (98)$$

$$1820 \leq 36R^2 \left(\frac{1}{n+1}\right)^{2/d}. \quad (99)$$

1829 \square

1831 **Lemma B.2.** *Let X takes values in $B(0, R)$. For all $d \geq 2$,*
1832

$$1833 \mathbb{E}[\|X_{(k)}(X) - X\|_2^2] \leq (2^{1+2/d})36R^2 \left(\frac{k}{n}\right)^{2/d}, \quad (100)$$

1835 where $X_{(k)}(X)$ is the nearest neighbor of X among X_1, \dots, X_n .

1836 *Proof of Lemma B.2.* Set $d \geq 2$. Recall that $\mathbb{E}[\|X_{(k)}(X) - X\|_2^2] \leq 4R^2$. Besides, for all $k > n/2$,
 1837 we have

$$1838 \quad (2^{1+2/d})36R^2 \left(\frac{k}{n}\right)^{2/d} > (2^{1+2/d})36R^2 \left(\frac{1}{2}\right)^{2/d} \quad (101)$$

$$1840 \quad > 72R^2 \quad (102)$$

$$1841 \quad > \mathbb{E}[\|X_{(k)}(X) - X\|_2^2]. \quad (103)$$

1842 Thus, the result is trivial for $k > n/2$. Set $k \leq n/2$. Now, following the argument of Theorem 2.4
 1843 in Biau & Devroye (2015), let us partition the set $\{X_1, \dots, X_n\}$ into $2k$ sets of sizes n_1, \dots, n_{2k}
 1844 with

$$1845 \quad \sum_{j=1}^{2k} n_j = n \quad \text{and} \quad \lfloor \frac{n}{2k} \rfloor \leq n_j \leq \lfloor \frac{n}{2k} \rfloor + 1. \quad (104)$$

1846 Let $X_{(1)}^*(j)$ be the nearest neighbor of X among all X_i in the j th group. Note that

$$1847 \quad \|X_{(k)}(X) - X\|^2 \leq \frac{1}{k} \sum_{j=1}^{2k} \|X_{(1)}^*(j) - X\|^2, \quad (105)$$

1848 since at least k of these nearest neighbors have values larger than $\|X_{(k)}(X) - X\|^2$. By Lemma B.1,
 1849 we have

$$1850 \quad \|X_{(k)}(X) - X\|^2 \leq \frac{1}{k} \sum_{j=1}^{2k} 36R^2 \left(\frac{1}{n_j + 1}\right)^{2/d} \quad (106)$$

$$1851 \quad \leq \frac{1}{k} \sum_{j=1}^{2k} 36R^2 \left(\frac{2k}{n}\right)^{2/d} \quad (107)$$

$$1852 \quad \leq 2^{1+2/d} \times 36R^2 \left(\frac{k}{n}\right)^{2/d}. \quad (108)$$

□

1853 *Proof of Corollary 3.6.* Let $d \geq 2$. By Markov's inequality, for all $\varepsilon > 0$, we have

$$1854 \quad \mathbb{P} [\|X_{(k)}(X) - X\|_2 > \varepsilon] \leq \frac{\mathbb{E}[\|X_{(k)}(X) - X\|_2^2]}{\varepsilon^2}. \quad (109)$$

1855 Let $\gamma \in (0, 1/d)$ and $\varepsilon = 12R(k/n)^\gamma$, we have

$$1856 \quad \mathbb{P} [\|X_{(k)}(X) - X\|_2 > 12R(k/n)^\gamma] \leq \left(\frac{k}{n}\right)^{2/d-2\gamma}. \quad (110)$$

1857 Noticing that, by construction of a SMOTE observation $Z_{K,n}$, we have

$$1858 \quad \|Z_{K,n} - X\|_2^2 \leq \|X_{(K)}(X) - X\|_2^2. \quad (111)$$

1859 Thus,

$$1860 \quad \mathbb{P} [\|Z_{K,n} - X\|_2^2 > 12R(k/n)^\gamma] \leq \mathbb{P} [\|X_{(K)}(X) - X\|_2^2 > 12R(k/n)^{1/d}] \quad (112)$$

$$1861 \quad \leq \left(\frac{k}{n}\right)^{2/d-2\gamma}. \quad (113)$$

□

1862 B.6 PROOF OF THEOREM 3.7

1863 *Proof of Theorem 3.7.* Let $\varepsilon > 0$ and $z \in B(0, R)$ such that $\|z\| \geq R - \varepsilon$. Let $A_\varepsilon = \{x \in$
 1864 $B(0, R), \langle x - z, z \rangle \leq 0\}$. Let $0 < \alpha < 2R$ and $\tilde{A}_{\alpha, \varepsilon} = A_\varepsilon \cap \{x, \|z - x\| \geq \alpha\}$. An illustration is
 1865 displayed in Figure 4.

1866 We have

$$1867 \quad f_Z(z) = \int_{x_c \in \tilde{A}_{\alpha, \varepsilon}} f_Z(z|X_c = x_c) f_X(x_c) dx_c + \int_{x_c \in \tilde{A}_{\alpha, \varepsilon}^c} f_Z(z|X_c = x_c) f_X(x_c) dx_c \quad (114)$$

1890
1891
1892
1893
1894
1895
1896
1897
1898
1899

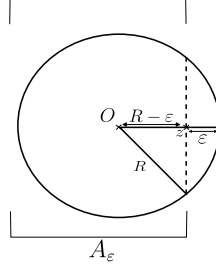


Figure 4: Illustration of Theorem 3.7.

1900
1901
1902

First term Let $x_c \in \tilde{A}_{\alpha, \varepsilon}$. In order to have $x_c + \frac{z-x_c}{w} = z + (-1 + \frac{1}{w})(z-x_c) \in B(0, R)$, it is necessary that

$$\left(-1 + \frac{1}{w}\right) \|z - x_c\| \leq \sqrt{2\varepsilon R} \quad (115)$$

1903
1904
1905
1906
1907
1908
1909

which leads to

$$w \geq \frac{1}{1 + \frac{\sqrt{2\varepsilon R}}{\|z-x_c\|}} \quad (116)$$

1910
1911
1912

Since $x_c \in \tilde{A}_{\alpha, \varepsilon}$, we have $\|x_c - z\| \geq \alpha$. Thus, according to inequality equation 116, $x_c + \frac{z-x_c}{w} \in B(0, R)$ implies

$$w \geq \frac{1}{1 + \frac{\sqrt{2\varepsilon R}}{\alpha}}. \quad (117)$$

1913
1914
1915
1916
1917
1918

Recall that $x_c + \frac{z-x_c}{w} \in \mathcal{X}$. Consequently, according to Lemma 3.3, for all $x_c \in \tilde{A}_{\alpha, \varepsilon}$,

$$f_Z(z|X_c = x_c) \quad (118)$$

1919
1920
1921
1922
1923

$$= (n-K-1) \binom{n-1}{K} \int_0^1 \frac{1}{w^d} f_X \left(x_c + \frac{z-x_c}{w} \right) \times \mathcal{B} \left(n-K-1, K; 1 - \mu_X \left(B \left(x_c, \frac{\|z-x_c\|}{w} \right) \right) \right) dw \quad (119)$$

1924
1925
1926
1927
1928

$$\leq C_2 (n-K-1) \binom{n-1}{K} \int_{\frac{1}{1 + \frac{\sqrt{2\varepsilon R}}{\alpha}}}^1 \frac{1}{w^d} \mathcal{B} \left(n-K-1, K; 1 - \mu_X \left(B \left(x_c, \frac{\|z-x_c\|}{w} \right) \right) \right) dw. \quad (120)$$

1929

Besides,

1930
1931
1932

$$(n-K-1) \binom{n-1}{K} \mathcal{B} \left(n-K-1, K; 1 - \mu_X \left(B \left(x_c, \frac{\|z-x_c\|}{w} \right) \right) \right) \quad (121)$$

1933
1934

$$= \left(\frac{n-1}{K} \right) (n-K-1) \binom{n-2}{K-1} \mathcal{B} \left(n-K-1, K; 1 - \mu_X \left(B \left(x_c, \frac{\|z-x_c\|}{w} \right) \right) \right) \quad (122)$$

1935
1936

$$\leq \frac{n-1}{K}, \quad (123)$$

1937

according to Lemma C.1. Thus,

1938
1939
1940

$$f_Z(z|X_c = x_c) \leq C_2 \left(\frac{n-1}{K} \right) \int_{\frac{1}{1 + \frac{\sqrt{2\varepsilon R}}{\alpha}}}^1 \frac{1}{w^d} dw \quad (124)$$

1941
1942
1943

$$\leq C_2 \left(\frac{n-1}{K} \right) \eta(\alpha, R), \quad (125)$$

1944 with

$$1945 \eta(\alpha, R) = \begin{cases} \ln\left(1 + \frac{\sqrt{2\varepsilon R}}{\alpha}\right) & \text{if } d = 1 \\ \frac{1}{d-1} \left(\left(1 + \frac{\sqrt{2\varepsilon R}}{\alpha}\right)^{d-1} - 1 \right) & \text{otherwise} \end{cases} .$$

1949 **Second term** According to Lemma 3.3, we have

$$1951 f_Z(z|X_c = x_c) = (n - K - 1) \binom{n-1}{K} \int_0^1 \frac{1}{w^d} f_X\left(x_c + \frac{z - x_c}{w}\right) \\ 1952 \times \mathcal{B}\left(n - K - 1, K; 1 - \mu_X\left(B\left(x_c, \frac{\|z - x_c\|}{w}\right)\right)\right) dw \quad (126)$$

$$1953 \leq \left(\frac{n-1}{K}\right) \int_0^1 \frac{1}{w^d} f_X\left(x_c + \frac{z - x_c}{w}\right) dw \quad (127)$$

1954 Since $\mathcal{X} \subset B(0, R)$, all points $x, z \in \mathcal{X}$ satisfy $\|x - z\| \leq 2R$. Consequently, if $\|z - x_c\|/w > 2R$,

$$1955 x_c + \frac{\|z - x_c\|}{w} \notin \mathcal{X}. \quad (128)$$

1961 Hence, for all $w \leq \|z - x_c\|/2R$,

$$1962 f_X\left(x_c + \frac{z - x_c}{w}\right) = 0. \quad (129)$$

1963 Plugging this equality into equation 127, we have

$$1964 f_Z(z|X_c = x_c) \quad (130)$$

$$1965 \leq \left(\frac{n-1}{K}\right) \int_{\|z-x_c\|/2R}^1 \frac{1}{w^d} f_X\left(x_c + \frac{z - x_c}{w}\right) dw \quad (131)$$

$$1966 \leq C_2 \left(\frac{n-1}{K}\right) \int_{\|z-x_c\|/2R}^1 \frac{1}{w^d} dw \quad (132)$$

$$1967 \leq C_2 \left(\frac{n-1}{K}\right) \left[-\frac{1}{d-1} w^{-d+1} \right]_{\|z-x_c\|/2R}^1 \quad (133)$$

$$1968 \leq C_2 \left(\frac{n-1}{K}\right) \frac{(2R)^{d-1}}{d-1} \frac{1}{\|z - x_c\|^{d-1}}. \quad (134)$$

1977 Besides, note that, for all $\alpha > 0$, we have

$$1978 \int_{B(z, \alpha)} \frac{1}{\|z - x_c\|^{d-1}} f_X(x_c) dx_c \quad (135)$$

$$1979 \leq C_2 \int_{B(0, \alpha)} \frac{1}{r^{d-1}} r^{d-1} \sin^{d-2}(\varphi_1) \sin^{d-3}(\varphi_2) \dots \sin(\varphi_{d-2}) dr d\varphi_1 \dots d\varphi_{d-2}, \quad (136)$$

1983 where $r, \varphi_1, \dots, \varphi_{d-2}$ are the spherical coordinates. A direct calculation leads to

$$1984 \int_{B(z, \alpha)} \frac{1}{\|z - x_c\|^{d-1}} f_X(x_c) dx_c \\ 1985 \leq C_2 \int_0^\alpha dr \int_{S(0, \alpha)} \sin^{d-2}(\varphi_1) \sin^{d-3}(\varphi_2) \dots \sin(\varphi_{d-2}) d\varphi_1 \dots d\varphi_{d-2} \quad (137)$$

$$1988 \leq \frac{2C_2 \pi^{d/2}}{\Gamma(d/2)} \alpha, \quad (138)$$

1991 as

$$1992 \int_{S(0, \alpha)} \sin^{d-2}(\varphi_1) \sin^{d-3}(\varphi_2) \dots \sin(\varphi_{d-2}) d\varphi_1 \dots d\varphi_{d-2} \quad (139)$$

1993 is the surface of the S^{d-1} sphere. Finally, for all $z \in \mathcal{X}$, for all $\alpha > 0$, and for all K, N such that $1 \leq K \leq N$, we have

$$1994 \int_{B(z, \alpha)} f_Z(z|X_c = x_c) f_X(x_c) dx_c \leq \frac{2C_2^2 (2R)^{d-1} \pi^{d/2}}{(d-1)\Gamma(d/2)} \left(\frac{n-1}{K}\right) \alpha. \quad (140)$$

Final result Using Figure 4 and Pythagore’s Theorem, we have $a^2 \leq \sqrt{2\varepsilon R}$. Let $d > 1$ and $\varepsilon > 0$. Then we have for all α such that $\alpha > a$.

$$f_Z(z) \tag{141}$$

$$= \int_{x_c \in \tilde{A}_{\alpha, \varepsilon}} f_Z(z|X_c = x_c) f_X(x_c) dx_c + \int_{x_c \in \tilde{A}_{\alpha, \varepsilon}^c} f_Z(z|X_c = x_c) f_X(x_c) dx_c \tag{142}$$

$$\leq \frac{C_2}{d-1} \left(\left(1 + \frac{\sqrt{2\varepsilon R}}{\alpha} \right)^{d-1} - 1 \right) \left(\frac{n-1}{K} \right) + \frac{2C_2^2(2R)^{d-1}\pi^{d/2}}{(d-1)\Gamma(d/2)} \left(\frac{n-1}{K} \right) \alpha \tag{143}$$

$$= \frac{C_2}{d-1} \left(\frac{n-1}{K} \right) \left[\left(\left(1 + \frac{\sqrt{2\varepsilon R}}{\alpha} \right)^{d-1} - 1 \right) + \frac{2C_2(2R)^{d-1}\pi^{d/2}}{\Gamma(d/2)} \alpha \right], \tag{144}$$

But this inequality is true if $\alpha \geq a$. We know that $(1+x)^{d-1} \leq (2^{d-1}-1)x+1$ for $x \in [0, 1]$ and $d-1 \geq 0$. Then, for α such that $\frac{\sqrt{2\varepsilon R}}{\alpha} \leq 1$,

$$f_Z(z) \tag{145}$$

$$\leq \frac{C_2}{d-1} \left(\frac{n-1}{K} \right) \left[\left(\left((2^{d-1}-1) \frac{\sqrt{2\varepsilon R}}{\alpha} + 1 \right) - 1 \right) + \frac{2C_2(2R)^{d-1}\pi^{d/2}}{\Gamma(d/2)} \alpha \right] \tag{146}$$

$$\leq \frac{C_2}{d-1} \left(\frac{n-1}{K} \right) \left[\left((2^{d-1}-1) \frac{\sqrt{2\varepsilon R}}{\alpha} \right) + \frac{2C_2(2R)^{d-1}\pi^{d/2}}{\Gamma(d/2)} \alpha \right]. \tag{147}$$

Since $\frac{\sqrt{2\varepsilon R}}{\alpha} \leq 1$, then $\alpha \geq \sqrt{2\varepsilon R} \geq a$. So our initial condition on α to get the upper bound of the second term is still true. Now, we choose α such that,

$$(2^{d-1}-1) \frac{\sqrt{2\varepsilon R}}{\alpha} \leq \frac{2C_2(2R)^{d-1}\pi^{d/2}}{\Gamma(d/2)} \alpha, \tag{148}$$

which leads to the following condition

$$\alpha \geq \left(\frac{\Gamma(d/2)(2^{d-1}-1)\sqrt{2\varepsilon R}}{2C_2(2R)^{d-1}\pi^{d/2}} \right)^{1/2}, \tag{149}$$

assuming that

$$\left(\frac{\varepsilon}{R} \right)^{1/2} \leq \frac{1}{\sqrt{2}dC_2} \text{Vol}(B_d(0, 1)). \tag{150}$$

Finally, for

$$\alpha = \left(\frac{\Gamma(d/2)(2^{d-1}-1)\sqrt{2\varepsilon R}}{2C_2(2R)^{d-1}\pi^{d/2}} \right)^{1/2}, \tag{151}$$

we have,

$$f_Z(z) \leq \frac{C_2}{d-1} \left(\frac{n-1}{K} \right) \left[\frac{4C_2(2R)^{d-1}\pi^{d/2}}{\Gamma(d/2)} \alpha \right] \tag{152}$$

$$\leq \frac{C_2}{d-1} \left(\frac{n-1}{K} \right) \left[\frac{4C_2(2R)^{d-1}\pi^{d/2}}{\Gamma(d/2)} \left(\frac{\Gamma(d/2)(2^{d-1}-1)\sqrt{2\varepsilon R}}{2C_2(2R)^{d-1}\pi^{d/2}} \right)^{1/2} \right] \tag{153}$$

$$= 2^{d+2} \left(\frac{n-1}{K} \right) \left(\frac{C_2^3 \text{Vol}(B_d(0, 1))}{d} \right)^{1/2} \left(\frac{\varepsilon}{R} \right)^{1/4}. \tag{154}$$

□

2052 C TECHNICAL LEMMAS

2053

2054

2055 C.0.1 CUMULATIVE DISTRIBUTION FUNCTION OF A BINOMIAL LAW

2056

2057

2058

2059

Lemma C.1 (Cumulative distribution function of a binomial distribution). *Let X be a random variable following a binomial law of parameter $n \in \mathbf{N}$ and $p \in [0, 1]$. The cumulative distribution function F of X can be expressed as Wadsworth et al. (1961):*

2060

2061

(i)

2062

2063

2064

2065

$$F(k; n, p) = \mathbb{P}(X \leq k) = \sum_{i=0}^{\lfloor k \rfloor} \binom{n}{i} p^i (1-p)^{n-i},$$

2066

2067

(ii)

2068

2069

2070

2071

2072

2073

$$\begin{aligned} F(k; n, p) &= (n-k) \binom{n}{k} \int_0^{1-p} t^{n-k-1} (1-t)^k dt \\ &= (n-k) \binom{n}{k} \mathcal{B}(n-k, k+1; 1-p), \end{aligned}$$

2074

2075

with $\mathcal{B}(a, b; x) = \int_{t=0}^x t^{a-1} (1-t)^{b-1} dt$, the incomplete beta function.

2076

2077

2078

Proof. see Wadsworth et al. (1961). □

2079

2080

2081 C.0.2 UPPER BOUNDS FOR THE INCOMPLETE BETA FUNCTION

2082

2083

2084

Lemma C.2. *Let $B(a, b; x) = \int_{t=0}^x t^{a-1} (1-t)^{b-1} dt$, be the incomplete beta function. Then we have*

2085

2086

2087

$$\frac{x^a}{a} \leq B(a, b; x) \leq x^{a-1} \left(\frac{1 - (1-x)^b}{b} \right),$$

2088

for $a > 0$.

2089

2090

Proof. We have

2091

2092

2093

2094

2095

2096

2097

2098

2099

2100

2101

2102

2103

2104

2105

$$\begin{aligned} B(a, b; x) &= \int_{t=0}^x t^{a-1} (1-t)^{b-1} dt \\ &\leq \int_{t=0}^x x^{a-1} (1-t)^{b-1} dt \\ &= x^{a-1} \int_{t=0}^x (1-t)^{b-1} dt \\ &= x^{a-1} \left[(-1) \frac{(1-t)^b}{b} \right]_0^x \\ &= x^{a-1} \left[-\frac{(1-x)^b}{b} + \frac{1}{b} \right] \\ &= x^{a-1} \frac{1 - (1-x)^b}{b}. \end{aligned}$$

2106 On the other hand,
2107

$$\begin{aligned}
 2108 \quad B(a, b; x) &= \int_{t=0}^x t^{a-1}(1-t)^{b-1} dt \\
 2109 & \\
 2110 &\geq \int_{t=0}^x x^{a-1} dt \\
 2111 & \\
 2112 &= \left[\frac{t^a}{a} \right]_0^x \\
 2113 & \\
 2114 &= \frac{x^a}{a} - \frac{0^a}{a} \\
 2115 & \\
 2116 &= \frac{x^a}{a}. \\
 2117 & \\
 2118 & \\
 2119 & \\
 2120 & \quad \square
 \end{aligned}$$

2123 C.0.3 UPPER BOUNDS FOR BINOMIAL COEFFICIENT

2124 **Lemma C.3.** For $k, n \in \mathbb{N}$ such that $k < n$, we have

$$2127 \quad \binom{n}{k} \leq \left(\frac{en}{k} \right)^k. \quad (155)$$

2131 *Proof.* We have,

$$2132 \quad \binom{n}{k} = \frac{n(n-1)\dots(n-k+1)}{k!} \leq \frac{n^k}{k!}. \quad (156)$$

2136 Besides,

$$2137 \quad e^k = \sum_{i=0}^{+\infty} \frac{k^i}{i!} \implies e^k \geq \frac{k^k}{k!} \implies \frac{e^k}{k^k} \geq \frac{1}{k!}. \quad (157)$$

2141 Hence,

$$2142 \quad \binom{n}{k} = \frac{n(n-1)\dots(n-k+1)}{k!} \leq \frac{n^k}{k!} \leq \left(\frac{en}{k} \right)^k. \quad (158)$$

2146 \square

2149 C.0.4 INEQUALITY $x \ln\left(\frac{1}{x}\right) \leq \sqrt{x}$

2150 **Lemma C.4.** For $x \in]0, +\infty[$,

$$2152 \quad x \ln\left(\frac{1}{x}\right) \leq \sqrt{x}. \quad (159)$$

2155 *Proof.* Let,

$$2157 \quad f(x) = \sqrt{x} - x \ln\left(\frac{1}{x}\right) \quad (160)$$

$$2158 \quad = \sqrt{x} + x \ln(x). \quad (161)$$

2160 Then,

$$2161 \quad f'(x) = \frac{1}{2\sqrt{x}} + \ln x + 1. \quad (162)$$

2164 And,

$$2165 \quad f''(x) = \frac{1}{x} - \frac{1}{4x^{3/2}}. \quad (163)$$

2168 We have,

$$2169 \quad f''(x) \geq 0 \implies \frac{1}{x} - \frac{1}{4x^{3/2}} \geq 0$$

$$2170 \quad \implies \frac{1}{x} \geq \frac{1}{4x^{3/2}} \quad (164)$$

2174 Since $x \in]0, +\infty[$,

$$2175 \quad \text{Equation (164)} \implies \frac{x^{3/2}}{x} \geq \frac{1}{4} \quad (165)$$

$$2176 \quad \implies \sqrt{x} \geq \frac{1}{4} \quad (166)$$

$$2177 \quad \implies x \geq \frac{1}{16}. \quad (167)$$

2182 This result leads to,

x	0	$\frac{1}{16}$	$+\infty$
f''	-	0	+
f'	\swarrow $2 + \ln\left(\frac{1}{16}\right) + 1$ \searrow		

(168)

2195 We have $2 + \ln\left(\frac{1}{16}\right) + 1 > 0$. So $f'(x) > 0$ for all $x \in]0, \infty[$. Furthermore $\lim_{x \rightarrow 0^+} f(x) = 0$,
 2196 hence $f(x) > 0$ for all $x \in]0, \infty[$, therefore $\sqrt{x} > x \ln\left(\frac{1}{x}\right)$ for all $x \in]0, \infty[$.

2198 □

2199
2200
2201
2202
2203
2204
2205
2206
2207
2208
2209
2210
2211
2212
2213